

AdS₃ spacetime genus fluctuations and their influence on the false vacuum decay

Hong Wang^a and Jin Wang^{b,1}

^a*State Key Laboratory of Electroanalytical Chemistry, Changchun Institute of Applied Chemistry, Chinese Academy of Sciences, Changchun 130022, China*

^b*Department of Chemistry and Department of Physics and Astronomy, State University of New York at Stony Brook, NY 11794, USA*

Abstract

In this work, we studied the genus fluctuations of the AdS₃ spacetime. The tunneling action of the high genus AdS₃ spacetime is formulated in the Siegel upper half space. Adopting the dilute wormhole gas approximation, we computed the genus creation rate in the semiclassical region. We show that a genus is more easily created in the spacetime corresponding to a larger absolute value of the cosmological constant. We find that fluctuations of fat wormholes are more likely to occur than those of thin wormholes. We also studied the influence of genus fluctuations on false vacuum decay. The vacuum decay rate will increase if the effect of genus fluctuations is included. We show that all results do not change qualitatively when the values of certain parameters are changed.

¹Corresponding author, jin.wang.1@stonybrook.edu

Contents

1	Introduction	2
2	Preliminaries	4
2.1	Schottky parametrization of the AdS_3 handlebody	4
2.2	Relationship between the period matrix and the Schottky group	7
3	The tunneling action	11
3.1	The total tunneling action and vacuum decay seed	11
3.2	Representing the tunneling action in the Siegel upper half space	20
4	Integration for the non-equivalent genus fluctuations	24
5	The tunneling rate	32
5.1	Genus creation rate	32
5.2	Genus fluctuations influence on the false vacuum decay	38
6	Conclusions and discussions	41

1 Introduction

The local properties of spacetime are determined by the metric, which can be obtained by solving the Einstein equations. Different spacetimes with identical metrics can exhibit varied topological structures. These structures are not determined by the Einstein equations. If one such spacetime is a solution of the Einstein equations, all others with different topologies but the same metric should also be solutions of the same equations. There is no reason to neglect these topologically non-trivial solutions. Moreover, the topological structures of spacetime may correspond to observable effects [1–3]. It is widely believed that quantum fluctuations can change the topological structures of spacetime [4–6]. Thus, the topological structures of spacetime are significant subjects in both classical and quantum gravity. One of the interesting spacetime topological structures is the genus.

The renormalization problem of four dimensional quantum gravity still has not been solved [7]. However, three dimensional quantum gravity is renormalizable and lacks bulk graviton excitations [8]. It has been proven that three dimensional Einstein pure gravity (with the exception of dark energy, there is no other matter) is equivalent to the Chern-Simons topological field theory [8]. Thus, three dimensions are an ideal case for studying topological issues in quantum gravity. Despite our universe being at least macroscopically four dimensional, insights from three dimensional studies are believed to offer valuable perspectives [6, 8].

When the cosmological constant is positive or zero, there is a finite class of topologically non-equivalent three dimensional spacetimes. However, in the case of the negative cosmological constant, there is an infinite class of topologically non-equivalent three dimensional spacetimes [9]. Thus, AdS_3 spacetime exhibits rich topological properties. The conformal boundary of the genus zero Euclidean AdS_3 spacetime is a cylinder. All genus one AdS_3 spacetimes are handlebodies. Higher genus AdS_3 spacetimes can be categorized as either handlebodies or non-handlebodies [10–12]. Some studies indicate that the contribution of non-handlebody spacetime to the partition function is small compared to that of handlebody spacetime [11, 12]. Therefore, for simplicity, we focus on the AdS_3 handlebody spacetime in this work.

Significant theoretical progress has been achieved in the study of spacetime with

a non-zero genus. In 1989, Witten showed that in the case where the cosmological constant is zero, the partition function of three dimensional pure quantum gravity can be expressed as the integration of the Ray-Singer analytic torsion over the moduli space of the Einstein equations [4]. In 1993, Carlip presented a method to compute the partition function of three dimensional pure quantum gravity, accounting for genus fluctuations. He showed that there is a divergence in the partition function [13]. In 2000, Krasnov demonstrated that the regularized Einstein-Hilbert action of the AdS_3 handlebody spacetime is equivalent to the Takhtajan-Zograf action, which is the action of the Liouville field defined on the two dimensional boundary of the bulk AdS_3 spacetime [14]. Following this, Takhtajan, Teo and Park proved that this equivalence holds even when the boundary surface exhibits elliptic or parabolic singularities (cone points or punctures, respectively) [15–17]. These findings strongly support the $\text{AdS}_3/\text{CFT}_2$ duality. In recent years, some researchers have employed new methods to study the partition function of thermal AdS_3 spacetime, incorporating the contributions of the boundary graviton excitations [18, 19]. Other significant studies have also been undertaken, see [20–27] and the references therein. We will not list them all here.

Although significant advances have been made in three dimensional topological quantum gravity, the challenge of genus fluctuations has still not been fully solved [4, 13]. In this work, we aim to study genus fluctuations of the AdS_3 spacetime. The Euclidean AdS_3 spacetime action is divergent and needs to be regularized [14]. We work on the semiclassical region and use the Euclidean path integral approach to compute the genus creation rate. We adopt the dilute wormhole gas approximation, facilitating the transformation of the tunneling action from the Schottky space to the Siegel upper half space. This approximation simplifies the issue of the integral domain, which is a subspace of the fundamental domain of the modular group $\text{Sp}(2g, \mathbb{Z})$ in the Siegel upper half space. Subsequently, integration over the physically non-equivalent AdS_3 spacetime becomes feasible. Our results indicate that the genus is easier to be created in the AdS_3 spacetime with a more negative cosmological constant. The genus creation is closely related to wormhole fluctuations. We find that fat wormhole fluctuations are more likely to occur than the thin ones.

We also studied the influence of genus fluctuations on AdS vacuum decay. Both

the dilute instanton gas approximation and the dilute wormhole gas approximation are used. Our analysis reveals that including genus fluctuations elevates the vacuum decay rate. We find that defining the initial state in our framework disrupts modular symmetry. Although there are two unspecified parameters in our model, we illustrate that the values of these parameters do not qualitatively change the results. Throughout this study, we work in units where $8\pi G = \hbar = k_B = c = 1$.

2 Preliminaries

2.1 Schottky parametrization of the AdS_3 handlebody

In this section, we briefly review some relevant mathematics for parameterizing the physically non-equivalent AdS_3 handlebody. The parameterization of the AdS_3 handlebody is essential for studying the genus fluctuations. Under a specific cosmological constant, the distinctions between various AdS_3 handlebodies are determined by their conformal boundaries. Thus, to parameterize the AdS_3 handlebody, one just needs to parameterize their conformal boundaries. The conformal boundary of any AdS_3 handlebody is a two dimensional closed Riemann surface. There are several different methods for parameterizing the two dimensional closed Riemann surface. Different parameterization methods may correspond to different ways of constructing the closed Riemann surface. We will focus on the Schottky parameterization. The mathematics reviewed in this section can be found in references [28, 29].

The Schottky group is a discrete subgroup of the two dimensional special complex linear transformation group $SL(2, \mathbb{C})$. The elements of the Schottky group can be expressed as

$$\mathcal{T} = \begin{pmatrix} a & b \\ c & d \end{pmatrix}. \quad (1)$$

The parameters a , b , c and d are complex numbers and satisfy $ad - bc = 1$. The Riemann sphere \mathbb{S} is a two dimensional complex sphere. The operation of the Schottky group on the Riemann sphere can be written as

$$\mathcal{T}(z) = \frac{az + b}{cz + d}. \quad (2)$$

Here, “ z ” represents a point on the Riemann sphere. We will use the symbol $\mathbf{Sch}(L_1, L_2, \dots, L_g)$ to represent the genus g Schottky group, where L_1, L_2, \dots, L_g represent its genera-

tors. $\mathbf{Sch}(L_1, L_2, \dots, L_g)$ is freely generated by L_1, L_2, \dots, L_g . That is, any element of $\mathbf{Sch}(L_1, L_2, \dots, L_g)$ can be written in the form $L_{r_1}^{n_1} L_{r_2}^{n_2} \dots L_{r_m}^{n_m}$, where $r_i = 1, 2, \dots, g$ and $n_i = \pm 1, \pm 2, \dots$

The operation of the generator of the Schottky group on the Riemann sphere can always be expressed as [30]

$$\frac{L_i(z) - \xi_i}{L_i(z) - \eta_i} = k_i \frac{z - \xi_i}{z - \eta_i}. \quad (3)$$

Here, $i = 1, 2, \dots, g$. ξ_i and η_i are the attractive fixed point and the repelling fixed point of the generator L_i , respectively. k_i is the multiplier, $|k_i| < 1$. The normalized Schottky group means $\xi_1 = 0$, $\xi_2 = 1$ and $\eta_1 = \infty$. The marked Schottky group means that the sets of generators L_1, L_2, \dots, L_g are ordered. Both the normalized and marked conditions are necessary in order to parameterize the two dimensional closed Riemann surface. In the latter, when we say Schottky group, we will always refer to the normalized and marked Schottky group.

Equation (3) indicates that $L_i(z)$ can be written as

$$L_i(z) = \frac{\eta_i(z - \xi_i) - k_i \xi_i(z - \eta_i)}{(z - \xi_i) - k_i(z - \eta_i)}. \quad (4)$$

Comparing equations (1), (2) and (4), one can read off the matrix representation of the generator L_i as

$$L_i = \frac{1}{\sqrt{|k_i|} |\eta_i - \xi_i|} \begin{pmatrix} \xi_i - k_i \eta_i & -\eta_i \xi_i (1 - k_i) \\ 1 - k_i & k_i \xi_i - \eta_i \end{pmatrix}. \quad (5)$$

According to equation (5), one can obtain the matrix representation of any element in the Schottky group $\mathbf{Sch}(L_1, L_2, \dots, L_g)$.

Denoting the multiplier of the element $L_i L_j$ as k_{ij} , then, it is proven that the relationship between k_{ij} and the parameters $(\xi_i, \eta_i, k_i, \xi_j, \eta_j, k_j)$ is [28]

$$k_{ij} = \frac{\det(L_i L_j)}{(\text{Tr}(L_i L_j))^2} + o(k_i^2, k_j^2) \approx k_i k_j \frac{(\eta_i - \xi_i)^2 (\eta_j - \xi_j)^2}{(\eta_j - \xi_i)^2 (\eta_i - \xi_j)^2}. \quad (6)$$

Here, $\det(L_i L_j)$ and $\text{Tr}(L_i L_j)$ represent the determinant and the trace of the element $L_i L_j$, respectively. $o(k_i^2, k_j^2)$ represents the higher order terms of the multipliers k_i and k_j . Note that $L_i(z)$ and $L_i^{-1}(z)$ have the same multiplier. Thus, according to equation (6), one can prove that the multiplier of the elements $L_i L_j$, $L_j L_i$, $L_i^{-1} L_j^{-1}$, $L_j^{-1} L_i^{-1}$ are equivalent to each other, and the multiplier of the elements $L_i^{-1} L_j$, $L_i L_j^{-1}$, $L_j^{-1} L_i$,

$L_j L_i^{-1}$ are also equivalent to each other [28]. Therefore, up to the first order of the multipliers, the Schottky group $\mathbf{Sch}(L_1, L_2, \dots, L_g)$ is approximated as

$$\mathbf{Sch}(L_1, L_2, \dots, L_g) \approx \{id, L_i, L_i^{-1} \mid i = 1, 2, \dots, g\}. \quad (7)$$

Here, id represents the identity element of the Schottky group. And the second order approximation is

$$\begin{aligned} \mathbf{Sch}(L_1, L_2, \dots, L_g) \approx \{ & id, L_i, L_i^{-1}, L_i L_j, L_i L_j^{-1}, L_i^{-1} L_j, L_i^{-1} L_j^{-1}, \\ & L_i^2, (L_i^{-1})^2 \mid i, j = 1, 2, \dots, g; i \neq j\}. \end{aligned} \quad (8)$$

Equation (3) indicates that L_i is determined by the parameters ξ_i, η_i and k_i . The genus g Schottky group $\mathbf{Sch}(L_1, L_2, \dots, L_g)$ is determined by its generators L_1, L_2, \dots, L_g . In addition, the normalized conditions of the Schottky group are $\xi_1 = 0, \xi_2 = 1$ and $\eta_1 = \infty$. Thus, a genus g Schottky group is determined by the set of parameters $(k_1, \eta_2, k_2, \xi_3, \eta_3, k_3, \dots, \xi_g, \eta_g, k_g)$. For the genus one Schottky group $\mathbf{Sch}(L_1)$, it only has one generator L_1 . Thus, it is determined by the parameters ξ_1, η_1, k_1 . However, ξ_1, η_1 are fixed by the normalized conditions. Therefore, the genus one Schottky group is completely determined by the multiplier k_1 .

Different sets of parameters $(k_1, \eta_2, k_2, \xi_3, \eta_3, k_3, \dots, \xi_g, \eta_g, k_g)$ correspond to various Schottky groups. All genus g ($g \geq 2$) Schottky groups form the genus g Schottky space. In the case of genus $g \geq 2$, the vector $(k_1, \eta_2, k_2, \xi_3, \eta_3, k_3, \dots, \xi_g, \eta_g, k_g)$ represents a point in the space \mathbb{C}^{3g-3} (\mathbb{C} is the complex plane). Thus, the dimension of the genus g ($g \geq 2$) Schottky space is equal to $6g - 6$. Similarly, the dimension of the genus one Schottky space is equal to two. Therefore, the dimension of the genus g Schottky space is equal to the dimension of the genus g Teichmüller space, which is composed of the conformal equivalence classes of the marked genus g Riemann surfaces. Furthermore, the Teichmüller space is the universal cover of the Schottky space.

Any closed Riemann surface can be constructed by the operation of the Schottky group on the Riemann sphere \mathbb{S} [14]:

$$\Sigma_g = (\mathbb{S} - \mathbf{Fix}) / \mathbf{Sch}(L_1, L_2, \dots, L_g). \quad (9)$$

Here, Σ_g represents the genus g closed Riemann surface. \mathbf{Fix} represents the set of the fixed points of the Schottky group. The fixed point of the element L of the Schottky

group is the point $z_0 \in \mathbb{S}$ that satisfies $L(z_0) = z_0$. $\mathbb{S} - \mathbf{Fix}$ represents the deletion of the fixed points from the Riemann sphere \mathbb{S} . Equation (9) represents the Schottky parameterization of the Riemann surface Σ_g . The Schottky parameterization of Σ_g models Σ_g as the quotient of $(\mathbb{S} - \mathbf{Fix})$ by the Schottky group $\mathbf{Sch}(L_1, L_2, \dots, L_g)$.

Equation (9) can be roughly interpreted in an intuitive way [14]. On the Riemann sphere \mathbb{S} , one can choose $2g$ non-intersecting circles $C_1, C'_1, C_2, C'_2, \dots, C_g, C'_g$ such that each circle lies outside of all the others. These circles are known as the Schottky circles. Cutting out the interior of each circle. Finally, gluing each pair of circles C_i and C'_i together to form a closed surface. The resulting surface is the Riemann surface Σ_g .

Equation (9) shows that a Schottky group corresponds to a Riemann surface Σ_g . Thus, every point in the Schottky space corresponds to a Riemann surface Σ_g . Therefore, the sets of parameters $(k_1, \eta_2, k_2, \xi_3, \eta_3, k_3, \dots, \xi_g, \eta_g, k_g)$ can be utilized to differentiate between different Riemann surfaces Σ_g . AdS₃ handlebody can be obtained by “filling” the interior of the Riemann surface Σ_g . Therefore, the Schottky space can be utilized to describe different AdS₃ handlebodies.

The Schottky space is useful for representing the regularized action of the AdS₃ handlebody. However, it is not quite convenient for summing the physically non-equivalent AdS₃ handlebody spacetime in the Schottky space. This is because different points in the Schottky space may correspond to the same Riemann surface, and the Schottky space is not simply connected [14]. For our model, the Siegel upper half space ($\mathbf{Sie}(g)$) is more convenient for summing different AdS₃ handlebodies.

2.2 Relationship between the period matrix and the Schottky group

The period matrix can also be used to distinguish between different Riemann surfaces Σ_g . It belongs to the elements of the space $\mathbf{Sie}(g)$. The relationship between the period matrix and the Schottky group can help to transform a function in the Schottky space into the space $\mathbf{Sie}(g)$. And the space $\mathbf{Sie}(g)$ is convenient for defining the integral region for integration over different AdS₃ handlebodies.

The generators of the homology group of the Riemann surface Σ_g are denoted as

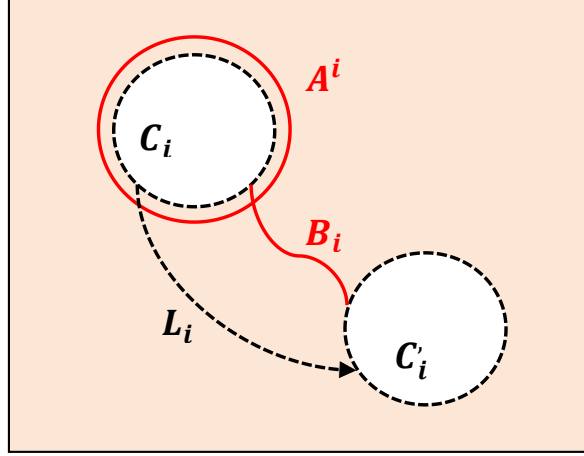


Figure 1: Diagram of the Schottky circles and the canonical homology bases of circles. The black dashed circles represent the Schottky circles. The red curves represent the canonical homology bases of circles. This figure is drawn on the Riemann sphere. The two ends of the curve B_i become the same point after the operation of the Schottky group.

$\{A^1, A^2, \dots, A^g; B_1, B_2, \dots, B_g\}$. All of them are non-contractible circles on Σ_g . Figure 1 depicts the relationship between the circles A^i , B_i and C_i , C'_i . A similar figure can be found in references [28, 31]. The definition of the period matrix is [32, 33]

$$\Pi(g)_{ij} \equiv \oint_{B_j} \omega_i, \quad (10)$$

where, ω_i is defined by [28, 29]

$$\omega_i \equiv \sum_{\mathcal{T} \in \mathbf{Sch}|L_i} \left(\frac{1}{z - \mathcal{T}(\eta_i)} - \frac{1}{z - \mathcal{T}(\xi_i)} \right) dz. \quad (11)$$

The symbol $\sum_{\mathcal{T} \in \mathbf{Sch}|L_i}$ represents that the sum is performed over all elements \mathcal{T} of the Schottky group $\mathbf{Sch}(L_1, L_2, \dots, L_g)$ that do not have L_i^n ($n = \pm 1, \pm 2, \dots$) as their right-most factor. ω_i is a holomorphic differential on the Riemann surface Σ_g . It is normalized along the A^i circle, that is, $\oint_{A^i} \omega_i = 2\pi i \delta_{ij}$.

Substituting equation (11) into (10), and completing the integration along the B_j circle, one can obtain [28, 29, 34]

$$2\pi i \Pi(g)_{ij} = \delta_{ij} \ln(k_i) + \sum_{\mathcal{T} \in L_i | \mathbf{Sch}|L_j} \ln \left(\frac{(\eta_i - \mathcal{T}(\eta_j))(\xi_i - \mathcal{T}(\xi_j))}{(\eta_i - \mathcal{T}(\xi_j))(\xi_i - \mathcal{T}(\eta_j))} \right). \quad (12)$$

Here, the symbol $\sum_{\mathcal{T} \in L_i | \mathbf{Sch}|L_j}$ represents that the sum is performed over all elements \mathcal{T} of the Schottky group $\mathbf{Sch}(L_1, L_2, \dots, L_g)$ that have neither L_i^n ($n = \pm 1, \pm 2, \dots$) as their

leftmost factor nor L_j^n as their rightmost factor. In the case where $i = j$, the identity element of $\mathbf{Sch}(L_1, L_2, \dots, L_g)$ is not included in the summation.

Equation (12) establishes the relationship between the period matrix and the Schottky group. However, it is difficult to calculate the summation on the right hand side of equation (12) strictly. In the latter, we will illustrate that the first order approximation (7) of the Schottky group $\mathbf{Sch}(L_1, L_2, \dots, L_g)$ is enough for our model. Under this approximation, only the elements $\{L_j, L_j^{-1} \mid j = 1, 2, \dots, g; j \neq i\}$ contribute to the summation in equation (12) when we calculate the element $\Pi(g)_{ii}$. For the calculation of the non-diagonal element $\Pi(g)_{ij}$ ($i \neq j$), one only needs to sum over the elements $\{id, L_n, L_n^{-1} \mid n = 1, 2, \dots, g; n \neq i; n \neq j\}$.

According to the discussions in the previous paragraph, the period matrix can be simplified to

$$2\pi i \Pi(g)_{ii} = \ln(k_i) + \sum_{n \neq i} \frac{2k_n(\xi_i - \eta_i)^2(\xi_n - \eta_n)^2}{(\xi_i - \xi_n)(\eta_i - \eta_n)(\eta_i - \xi_n)(\xi_i - \eta_n)} + \sum_{n \neq i} o(k_n^2), \quad (13)$$

$$2\pi i \Pi(g)_{ij} = \ln \frac{(\eta_i - \eta_j)(\xi_i - \xi_j)}{(\eta_i - \xi_j)(\xi_i - \eta_j)} + \sum_{n \neq i, j} \frac{2k_n(\xi_n - \eta_n)^2(\eta_i - \xi_i)(\eta_j - \xi_j)}{(\eta_i - \xi_n)(\xi_i - \xi_n)(\eta_j - \eta_n)(\xi_j - \eta_n)} + \sum_{n \neq i, j} o(k_n^2). \quad (14)$$

In equation (13), $n = 1, 2, \dots, g$ and $n \neq i$. In equation (14), $n = 1, 2, \dots, g$ and $n \neq i, j$. From equation (12) to (13) and (14), we have used the formula [28]

$$\frac{(z_1 - L_i(\sigma_1))(z_2 - L_i(\sigma_2))}{(z_1 - L_i(\sigma_2))(z_2 - L_i(\sigma_1))} = 1 + \frac{k_i(\xi_i - \eta_i)^2(z_1 - z_2)(\sigma_1 - \sigma_2)}{(z_1 - \xi_i)(z_2 - \xi_i)(\sigma_1 - \eta_i)(\sigma_2 - \eta_i)} + o(k_i^2). \quad (15)$$

Here, z_1, z_2, σ_1 and σ_2 are points on the Riemann surface Σ_g . In the case where the Schottky group only has two generators, equations (13) and (14) will reduce to equation (A.28) in reference [28].

Different AdS_3 handlebody spacetimes can be characterized by the period matrix. For instance, the conformal boundary of the Euclidean thermal AdS_3 spacetime (TAdS₃) is a torus. The period matrix of a torus is a complex number, that is the modular parameter of the torus. The real part of the period matrix of the TAdS₃ corresponds to the angular potential, while its imaginary part corresponds to the inverse of temperature. The time circle (a circle where different points on the circle correspond to different times.) of the TAdS₃ is non-contractible. Figure 2 (a) illustrates that a wormhole is

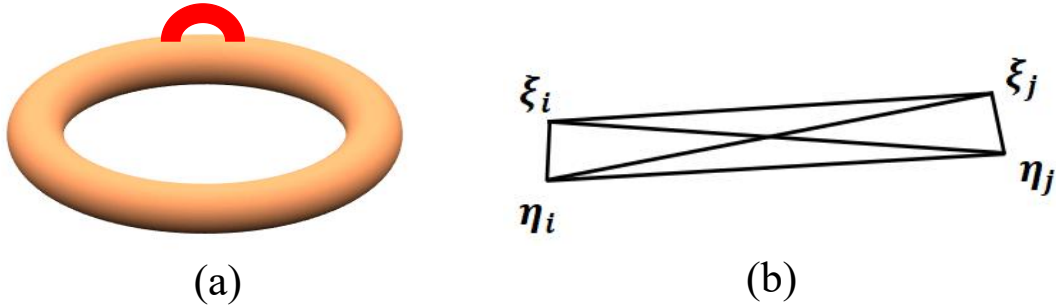


Figure 2: Diagram of the wormhole fluctuations and the dilute wormhole gas approximation. Figure 2 (a) depicts the wormhole fluctuations. Figure 2 (b) illustrates the dilute wormhole gas approximation. In figure 2 (a), the orange torus represents the conformal boundary of a Euclidean thermal AdS_3 spacetime. The red strip represents a wormhole with two ends. In figure 2 (b), ξ_i and η_i approximately denotes the two ends of a wormhole, while ξ_j and η_j represent the two ends of another wormhole.

created in the TAdS_3 . This process of wormhole fluctuation gives rise to a genus, which can also be referred to as genus fluctuation. The resulting spacetime is a genus two handlebody, with the period matrix being a 2×2 symmetric matrix. We pointed out that in this work, the terms wormhole fluctuations and genus fluctuations refer to the same phenomenon. We use these terms interchangeably.

Equations (13) and (14) are still complicated. We need to simplify them further. To achieve this, we will consider the dilute wormhole gas approximation [35, 36]. This implies that the size of the wormhole is much smaller than their distance. Noted that under the small k_i limit, ξ_i and η_i approximately represent the two ends of the wormhole [37]. Thus, in this case, one can use the equation

$$|\xi_i - \eta_i| \ll |\xi_i - \eta_j| \quad (i \neq j) \quad (16)$$

to represent the dilute wormhole gas approximation. Figure 2 (b) depicts the dilute wormhole gas approximation visually. It also illustrates that the differences between $|\xi_i - \eta_j|$, $|\xi_i - \xi_j|$ and $|\eta_i - \eta_j|$ ($i \neq j$) are small.

Using equation (16), the period matrix in equations (13) and (14) can be approximated to

$$2\pi i \Pi(g)_{ii} \approx \ln(k_i), \quad (17)$$

$$2\pi i \Pi(g)_{ij} \approx \ln \frac{(\eta_i - \eta_j)(\xi_i - \xi_j)}{(\eta_i - \xi_j)(\xi_i - \eta_j)}. \quad (18)$$

Equations (17) and (18) represent the relationships between the period matrix and the

Schottky group under the dilute wormhole gas approximation. These two equations are consistent with the formula (3.3) in references [37].

Following the discussions of Lyons and Hawking in reference [37], if the generators L_i and L_j correspond to two different wormholes, then the element $\Pi(g)_{ij}$ ($i \neq j$) can be interpreted as the interaction between wormhole i and j . Thus, equation (18) indicates that the interaction between different wormholes is small under the dilute wormhole gas approximation. A special situation is that all the non-diagonal elements of the period matrix are zero. In this case, $\Pi(g) = \Pi(g)_{11} \oplus \Pi(g)_{22} \oplus \cdots \oplus \Pi(g)_{gg}$. It represents a set of separated tori, where the modular parameter of the i th torus is $\Pi(g)_{ii}$.

The Siegel upper half space $\mathbf{Sie}(g)$ consists of all $g \times g$ symmetric matrices in which the imaginary part of any matrix element is positive [38]. In other words, the space $\mathbf{Sie}(g)$ is defined as $\mathbf{Sie}(g) \equiv \{\Omega \mid \Omega_{ij} = \Omega_{ji}, \text{Im}(\Omega_{ij}) > 0\}$. The $g \times g$ period matrix is also symmetric ($\Pi(g)_{ij} = \Pi(g)_{ji}$) and belongs to the elements of the space $\mathbf{Sie}(g)$. Equations (17) and (18) can be used to transform the tunneling action from the Schottky space into the space $\mathbf{Sie}(g)$. This helps to sum over different AdS₃ handlebodies.

3 The tunneling action

3.1 The total tunneling action and vacuum decay seed

The Euclidean action of the real scalar field coupled with the three dimensional space-time is [40]

$$S_E = \int dx^3 \sqrt{g} \left\{ -\frac{1}{2}R + \frac{1}{2}g^{\mu\nu} \partial_\mu \phi \partial_\nu \phi + V(\phi) \right\} + S_{GHY}. \quad (19)$$

Here, S_E represents the Euclidean action of the total system. R and S_{GHY} represent the Ricci scalar and the Gibbons-Hawking-York surface term, respectively. ϕ represents the scalar field, and $V(\phi)$ represents the scalar potential. In our model, the scalar potential has two minimal values, as shown in figure 3. These minimal values are labeled as $V(\phi_1)$ and $V(\phi_2)$ with $V(\phi_1) < V(\phi_2) < 0$. Thus, when the scalar field is in the state $V(\phi_1)$ or $V(\phi_2)$, the spacetime is AdS₃ spacetime. For simplicity, we assume $\epsilon = V(\phi_2) - V(\phi_1)$ to be a small quantity. In this case, the thin wall approximation is valid [41, 42]. The generation to the scenario where the potential has more local minima is straightforward.

For the homogenous and isotropic spacetime ($k = 1$), its local properties are deter-

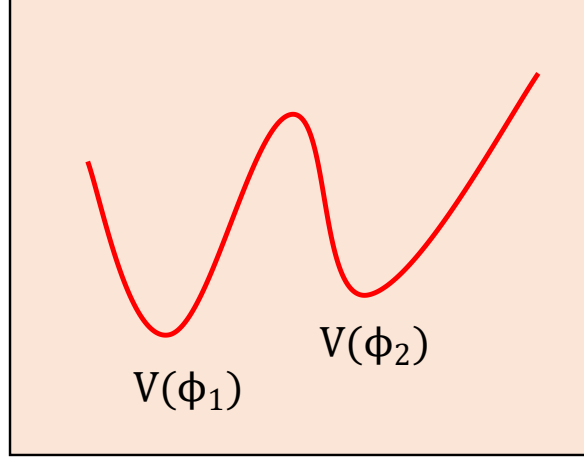


Figure 3: Diagram of the scalar potential. It has two minimal values, denoted as $V(\phi_1)$ and $V(\phi_2)$.

mined by the metric [40]

$$ds^2 = d\tau_E^2 + \rho(\tau_E)^2(d\theta^2 + \sin^2\theta d\varphi^2). \quad (20)$$

Here, τ_E and $\rho(\tau_E)$ represent the Euclidean proper time and the scale factor, respectively. The parameters φ and θ have a value range of $0 \leq \varphi \leq 2\pi$ and $0 \leq \theta \leq \pi$, respectively. The Ricci scalar is [40]

$$R = -4\frac{\ddot{\rho}}{\rho} + \frac{2}{\rho^2}(1 - \dot{\rho}^2), \quad (21)$$

where, $\dot{\rho} \equiv d\rho/d\tau_E$.

Substituting equations (20) and (21) into (19), and completing the integration over the variables θ and φ , then the Euclidean action S_E becomes

$$S_E = 4\pi \int d\tau_E \left\{ -(1 + \dot{\rho}^2) + \rho^2 \left[\frac{1}{2} \dot{\phi}^2 + V(\phi) \right] \right\}. \quad (22)$$

From equation (19) to (22), we have used the fact that the Gibbons-Hawking-York surface term S_{GHY} is canceled out by the boundary term generated in the partial integral with respect to the Ricci scalar R .

Based on equation (22), one can obtain that the total Hamiltonian (H_{tot}) of the system is

$$H_{tot} = -4\pi\dot{\rho}^2 + 2\pi\rho^2\dot{\phi}^2 - 4\pi\rho^2V(\phi) + 4\pi. \quad (23)$$

The general covariance implies that the total Hamiltonian must be equal to zero [42–45]. Taking $\delta S_E/\delta\phi = 0$ and $H_{tot} = 0$, one can obtain the dynamical equations [40]

$$\ddot{\phi} = \frac{\partial V}{\partial\phi}, \quad (24)$$

$$\dot{\rho}^2 = 1 + \rho^2\left(\frac{1}{2}\dot{\phi}^2 - V(\phi)\right). \quad (25)$$

Equation (24) is the Klein-Gordon equation, while equation (25) is the Friedmann equation. Noted that on the left side of equation (24), we have neglected the Hubble drag term $2\dot{\rho}\dot{\phi}/\rho$ as it is small under the thin wall approximation [41]. Using equation (25), the Euclidean action (22) can be simplified to

$$S_E = 8\pi \int d\tau_E \{ -1 + \rho^2 V(\phi) \}. \quad (26)$$

It is possible for the false vacuum state $V(\phi_2)$ to decay into the true vacuum state $V(\phi_1)$. According to the Coleman-De Luccia theory, the vacuum decay rate is given by [41]

$$\Gamma \approx \exp\{ - (S_E(\phi_{bounce}) - S_E(\phi_2)) \} \equiv e^{-B}. \quad (27)$$

Here, ϕ_{bounce} represents the bounce solution of equation (24). We refer to $S_E(\phi_2)$ as the background term and B as the total tunneling action. When deriving equation (27), both the semiclassical approximation and the dilute instanton gas approximation are used.

Under the thin wall approximation, the bounce solution can be seen as a three dimensional sphere symmetric bubble (the bounce bubble) embedded in a sea of false vacuum. The radius of the bounce bubble $\bar{\rho}$ is determined by the condition $\partial B/\partial\bar{\rho} = 0$. Thus, the tunneling action can be written as $B = B_{in} + B_{wall} + B_{out}$, where B_{in} and B_{out} denote the tunneling action inside and outside the bubble, respectively. And B_{wall} represents the tunneling action on the domain wall.

Inside the bubble, $\phi_{bounce} = \phi_1$, $\dot{\phi} = 0$ and $d\rho = \sqrt{1 - \rho^2 V(\phi_1)} d\tau_E$ (this relationship can be derived from equation (25) by setting $\dot{\phi} = 0$). Combining equations (26) and (27) with these conclusions, one can easily show that the tunneling action B_{in} is

$$B_{in} = -8\pi \int_0^{\bar{\rho}} d\rho [1 - \rho^2 V(\phi_1)]^{\frac{1}{2}} + 8\pi \int_0^{\bar{\rho}} d\rho [1 - \rho^2 V(\phi_2)]^{\frac{1}{2}}. \quad (28)$$

Using the integral formula

$$\int_0^a \sqrt{1 - bx^2} dx = \frac{1}{2} \{ a\sqrt{1 - a^2b} + b^{-\frac{1}{2}} \arcsin(a\sqrt{b}) \}, \quad (29)$$

performing the integral over the variable ρ , then equation (28) becomes

$$B_{in} = 4\pi \{ V^{-\frac{1}{2}}(\phi_2) \arcsin(\bar{\rho}\sqrt{V(\phi_2)}) - V^{-\frac{1}{2}}(\phi_1) \arcsin(\bar{\rho}\sqrt{V(\phi_1)}) \} \\ + 4\pi\bar{\rho} \{ \sqrt{1 - \bar{\rho}^2V(\phi_2)} - \sqrt{1 - \bar{\rho}^2V(\phi_1)} \}. \quad (30)$$

Equation (30) is the tunneling action inside the bubble.

The tension (μ) of the domain wall is $\mu = \int_{\phi_1}^{\phi_2} d\phi \sqrt{2(V(\phi) - V(\phi_2))}$ [42, 46]. Under the thin wall approximation, the tension μ and the tunneling action B_{wall} are equal to the energy density and the total energy of the domain wall, respectively [47]. Therefore, the tunneling action B_{wall} is

$$B_{wall} = 4\pi\bar{\rho}^2\mu = 4\pi\bar{\rho}^2 \int_{\phi_1}^{\phi_2} d\phi \sqrt{2(V(\phi) - V(\phi_2))}. \quad (31)$$

Equation (31) is the lower dimensional version of equation (2.15) in reference [41]. Outside the bubble, $\phi_{bounce} = \phi_2$. Thus, in the case where there are no genus fluctuations, $B_{out} = 0$. A more detailed explanation of this method for calculating tunneling action can be referenced in [41].

For convenience, we define

$$B_{seed} \equiv B_{in} + B_{wall}. \quad (32)$$

as the vacuum decay seed. Therefore, if there are no genus fluctuations, $B = B_{seed}$. However, if there are genus fluctuations, $B_{out} \neq 0$. Thus, in this scenario, $B \neq B_{seed}$. To illustrate this result, we initially categorize the genus fluctuations into three classes. In the first class, both ends of the wormhole are inside the bubble. In the second class, one end of the wormhole is inside the bubble, while the other end is outside the bubble. In the third class, both ends of the wormhole are outside the bubble.

The size of the bubble can be neglected compared to the size of the AdS₃ spacetime. Therefore, the predominant genus fluctuations belong to the third class. Consequently, the first and second class of genus fluctuations can be neglected. The third class of genus fluctuations is independent of the bounce bubble, thus it does not change the

vacuum decay seed B_{seed} . However, it can impact the volume outside the bubble, thereby affecting the tunneling action B_{out} .

Noted that equation (26) can be equivalently written as

$$S_E = 2 \int dx^3 \sqrt{g} \left\{ \frac{-1}{\rho^2} + V(\phi) \right\}. \quad (33)$$

Typically, in high genus spacetime, $\int dx^3 \sqrt{g} \neq 4\pi \int \rho^2 d\tau_E$, so equation (26) is not applicable. However, equations (20), (21) and (25) remain correct in high genus spacetime. Hence, equation (33) holds true in high genus spacetime.

If there are no genus fluctuations, the tunneling action B_{out} can be expressed as

$$B_{out} = 2 \int_{\rho > \bar{\rho}; g=0} dx^3 \sqrt{g} \left\{ \frac{-1}{\rho^2} + V(\phi_{bounce} = \phi_2) \right\} - 2 \int_{\rho > \bar{\rho}; g=0} dx^3 \sqrt{g} \left\{ \frac{-1}{\rho^2} + V(\phi_2) \right\} \quad (34)$$

$$= 0.$$

Here, the symbol $\int_{\rho > \bar{\rho}; g=0}$ represents that the integration is performed over the exterior of the bubble. $g = 0$ represents that the genus of the spacetime is zero. The equation (33) is applicable for high genus spacetime. Taking into consideration the genus fluctuations, the tunneling action B_{out} should be modified as

$$B_{out} = 2 \int_{\rho > \bar{\rho}; g=n} dx^3 \sqrt{g} \left\{ \frac{-1}{\rho^2} + V(\phi_2) \right\} - 2 \int_{\rho > \bar{\rho}; g=0} dx^3 \sqrt{g} \left\{ \frac{-1}{\rho^2} + V(\phi_2) \right\}. \quad (35)$$

Equation (35) has two terms on the right hand side. The first term corresponds to a spacetime with the genus $g = n$. The genus is generated by the genus fluctuations. The second term is the background term, unaffected by the genus fluctuations. The first term is not equal to the second term, hence the genus fluctuations result in $B_{out} \neq 0$.

Under the thin wall approximation, the bubble radius $\bar{\rho} \gg 0$. Thus, when $\rho > \bar{\rho}$, one can expect that $1/\rho^2 \rightarrow 0$. As a result, equation (35) can be approximated as

$$B_{out} \approx 2 \int_{\rho > \bar{\rho}; g=n} dx^3 \sqrt{g} V(\phi_2) - 2 \int_{\rho > \bar{\rho}; g=0} dx^3 \sqrt{g} V(\phi_2). \quad (36)$$

We have illustrated that the region $\rho < \bar{\rho}$ is not altered by the third class of genus fluctuations (the first and second classes can be neglected). Thus, the tunneling action B_{out} is equal to

$$B_{out} = 2V(\phi_2) \left\{ \int_{g=n} dx^3 \sqrt{g} - \int_{g=0} dx^3 \sqrt{g} \right\}. \quad (37)$$

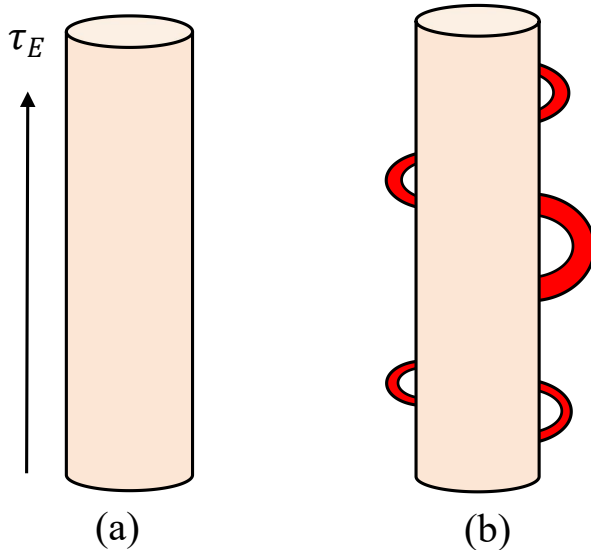


Figure 4: The conformal boundary of the genus zero AdS₃ spacetime and the high genus handlebody spacetime. In figure 4 (a) and (b), the cylinder represents the parent universe. In figure 4 (b), the red strips represent the wormholes.

On the right hand side of equation (37), the integrations are performed over the entire spacetime. The factor $\int_{g=n} dx^3 \sqrt{g}$ represents the volume of the AdS₃ spacetime with the genus $g = n$. And $\int_{g=0} dx^3 \sqrt{g}$ is the volume of the genus zero AdS₃ spacetime.

Figure 4 depicts the genus fluctuations. The cylinder in figure 4 (a) and (b) represents the parent universe, which is a genus zero AdS₃ spacetime. The red strips in figure 4 (b) represent the wormholes. On the right hand side of equation (37), the factor $\int_{g=n} dx^3 \sqrt{g}$ corresponds to the spacetime in figure 4 (b), while the factor $\int_{g=0} dx^3 \sqrt{g}$ corresponds to the spacetime in figure 4 (a). Both $\int_{g=n} dx^3 \sqrt{g}$ and $\int_{g=0} dx^3 \sqrt{g}$ are infinite. Usually, one use the regularized volume to replace them. We denote the regularized volume of the AdS₃ spacetime with the genus $g = n$ as $Rvol(g = n)$. Then, equation (37) should be modified as

$$B_{out} = 2V(\phi_2) \{Rvol(g = n) - Rvol(g = 0)\}. \quad (38)$$

In this study, we only focus on the physics at zero temperature. Physically, as the temperature (T) of the TAdS₃ approaches zero, the TAdS₃ transforms into the zero temperature AdS₃ spacetime with a conformal boundary in the shape of a cylinder, as shown in figure 4 (a). Therefore, it is natural to consider that $\lim_{T \rightarrow 0} \text{TAdS}_3$ is equivalent to the genus zero parent universe depicted in figure 4 (a). Hence, for convenience, we will

use $\lim_{T \rightarrow 0} \text{TAdS}_3$ to define the genus zero parent universe. Furthermore, we will denote $V(\phi, T)$ as the scalar potential in the TAdS_3 (the temperature may influence the scalar potential) and set $\lim_{T \rightarrow 0} V(\phi, T)$ to be equal to the scalar potential $V(\phi)$ in equation (19).

The genus of the TAdS_3 is one. We use $Rvol_T(g = 1)$ to denote the regularized volume of the TAdS_3 . Then, the term $2V(\phi_2)Rvol(g = 0)$ in equation (38) can be expressed as

$$2V(\phi_2)Rvol(g = 0) = 2 \lim_{T \rightarrow 0} \left(V(\phi_2, T) \cdot Rvol_T(g = 1) \right). \quad (39)$$

We also use $Rvol_T(g = n+1)$ to represent the regularized volume of the spacetime where the parent universe is the TAdS_3 and the genus generated by the genus fluctuations is n . And $g = n + 1$ is the total genus of the AdS_3 handlebody. Subsequently, the term $2V(\phi_2)Rvol(g = n)$ in equation (38) can be represented as

$$2V(\phi_2)Rvol(g = n) = 2 \lim_{T \rightarrow 0} \left(V(\phi_2, T) \cdot Rvol_T(g = n + 1) \right). \quad (40)$$

Hence, equation (38) can be rewritten as

$$B_{out} = 2 \lim_{T \rightarrow 0} \left\{ V(\phi_2, T) \cdot \left(Rvol_T(g = n + 1) - Rvol_T(g = 1) \right) \right\}. \quad (41)$$

In equation (41), when $n = 0$, $B_{out} = 0$. This corresponds to the case where there are no genus fluctuations.

The regularized volume of the AdS_3 handlebody can be obtained from the regularized Euclidean Einstein-Hilbert action of the AdS_3 spacetime, defined as [12, 14]

$$I_{reg} \equiv -\frac{1}{2} \int dx^3 \sqrt{g} (R - 2\Lambda) + 2 \int dx^2 \sqrt{\gamma} (K - \sqrt{-\Lambda}) + Count.. \quad (42)$$

Here, Λ represents the cosmological constant ($\Lambda < 0$). K and γ represent the trace of the extrinsic curvature and the induced metric on the boundary, respectively. The term *Count.* represents the counterterm for removing the logarithmic divergence [14]. The details discussion about this counterterm can be found in [12]. The regularized action (42) and the Euclidean Einstein-Hilbert action $-\int dx^3 \sqrt{g} (R/2 - \Lambda)$ correspond to the same dynamical equation.

In [14], Krasnov demonstrated that the regularized action I_{reg} can be simplified to

$$I_{reg} = 2\pi \sqrt{\frac{-1}{\Lambda}} (\ln|k_1| + \ln \rho_2 \rho_2' \cdots \rho_g \rho_g'), \quad (43)$$

where ρ_i (ρ'_i) represents the radius of the Schottky circle C_i (C'_i). And k_1 is the multiplier of the generator L_1 of the Schottky group $\mathbf{Sch}(L_1, L_2, \dots, L_g)$. In the case of $g = 1$, the regularized action $I_{reg} = 2\pi\sqrt{-1/\Lambda}\ln|k_1|$. This is the regularized action of the TAdS₃ [14]. Thus, the variable k_1 and the generator L_1 correspond to the TAdS₃. The action of the BTZ black hole can also be represented as the regularized action I_{reg} with $g = 1$ [14]. The distinction between TAdS₃ and the BTZ black hole lies in the fact that for the TAdS₃, the time circle is non contractible, whereas for the BTZ black hole, the time circle is contractible [14].

Equation (43) can also be derived from the Takhtajan-Zograf action, which is defined as [12, 14, 48]

$$I_{TZ} = \frac{1}{2}\sqrt{\frac{-1}{\Lambda}} \left\{ \iint_{F_S} \frac{i}{2} dz \wedge d\bar{z} (4\partial_z \psi \partial_{\bar{z}} \psi + \frac{1}{2} e^{2\psi}) + i \int_{C_j} \sum_{j=2}^g (d\bar{z} \psi \frac{\partial_z^2 \bar{L}_j}{\partial_z \bar{L}_j} - dz \psi \frac{\partial_z^2 L_j}{\partial_z L_j}) \right. \\ \left. + \frac{i}{2} \int_{C_j} \sum_{j=2}^g \ln |\partial_z L_j|^2 \frac{\partial_z^2 L_j}{\partial_z L_j} dz + 4\pi \sum_{j=2}^g \ln |(L_j)_{21}|^2 \right\}. \quad (44)$$

Here, I_{TZ} and ψ represent the Takhtajan-Zograf action and the Liouville conformal field, respectively. C_j and F_S represent the Schottky circle and the fundamental domain of the Schottky group $\mathbf{Sch}(L_1, L_2, \dots, L_g)$ acting on the Riemann sphere \mathbb{S} , respectively. \bar{z} and \bar{L}_j represent the complex conjugate of z and L_j , respectively. And $(L_j)_{21}$ represents the element of the second row and first column of the generator L_j . Equation (5) indicates that $(L_j)_{21} = (1 - k_j)/(\sqrt{|k_j|}|\xi_j - \eta_j|)$. The Takhtajan-Zograf action is the action of the Liouville conformal field theory defined on the conformal boundary of the AdS₃ handlebody spacetime.

The relationship between the radius of the Schottky circle and the parameters (ξ_i, η_i, k_i) is [28, 37]

$$\rho_i = \rho'_i = \left| \frac{\sqrt{k_i}(\xi_i - \eta_i)}{1 - k_i} \right|. \quad (45)$$

Therefore, the regularized action I_{reg} can be expressed as

$$I_{reg} = 2\pi\sqrt{\frac{-1}{\Lambda}} \left\{ \ln|k_1| + 2\ln \left| \frac{\sqrt{k_2}(\xi_2 - \eta_2)}{1 - k_2} \frac{\sqrt{k_3}(\xi_3 - \eta_3)}{1 - k_3} \dots \frac{\sqrt{k_g}(\xi_g - \eta_g)}{1 - k_g} \right| \right\}. \quad (46)$$

The normalized condition of the Schottky group implies that $\xi_2 = 1$. Equation (46) clearly indicates that the regularized action I_{reg} is a $(6g - 6)$ -variate function in the

Schottky space. The variables are $(k_1, \eta_2, k_2, \xi_3, \eta_3, k_3, \dots, \xi_g, \eta_g, k_g)$ with $g \geq 2$. In the case of $g = 1$, the unique variable of I_{reg} is k_1 . The variable k_1 describes the properties of the TAdS₃. Other variables $(\eta_2, k_2, \xi_3, \eta_3, k_3, \dots, \xi_g, \eta_g, k_g)$ describe the properties of the wormholes. The meaning of these parameters are presented in section 2.1.

Recalling that for the TAdS₃, the relationship between the regularized action and the regularized volume $Rvol_T(g = 1)$ is $I_{reg} = -2\Lambda \cdot Rvol_T(g = 1)$. This relationship can be easily extended to any genus AdS₃ spacetime: $I_{reg} = -2\Lambda \cdot Rvol(g = n)$. Therefore, based on equation (46), the regularized volume $Rvol_T(g = n + 1)$ can be represented as

$$Rvol_T(g = n + 1) = -\frac{\pi}{\Lambda} \sqrt{\frac{-1}{\Lambda}} \left\{ \ln|k_1| + 2\ln \left| \frac{\sqrt{k_2}(1 - \eta_2)}{1 - k_2} \right| + 2\ln \left| \frac{\sqrt{k_3}(\xi_3 - \eta_3)}{1 - k_3} \dots \frac{\sqrt{k_g}(\xi_g - \eta_g)}{1 - k_g} \right| \right\}. \quad (47)$$

The term $-\pi\Lambda^{-1}\sqrt{-\Lambda^{-1}}\ln|k_1|$ in equation (47) represents the regularized volume of the TAdS₃.

Assuming the period matrix of the TAdS₃ is $\Pi(1)$. For the genus one handlebody, $\Pi(1)$ is equal to the modular parameter of the torus. Equation (17) shows that $2\pi i\Pi(1) = \ln k_1$. Furthermore, the inverse of the temperature ($\frac{1}{T}$) of the TAdS₃ is proportional to the imaginary part of $\Pi(1)$ [14, 49]. Therefore, $\frac{1}{T} \propto \ln|k_1|$. Other parameters $(\eta_2, k_2, \xi_3, \eta_3, k_3, \dots, \xi_g, \eta_g, k_g)$ are independent of the multiplier k_1 , hence they are also independent of the temperature T . The term proportional to the factor $\ln|k_1|$ in equation (47) is cancelled by the term $Rvol_T(g = 1)$ in equation (41). Combining equation (47) with this conclusion, equation (41) can be written as

$$B_{out} = -4\pi \sqrt{\frac{-1}{V(\phi_2)}} \left\{ \ln \left| \frac{\sqrt{k_2}(1 - \eta_2)}{1 - k_2} \frac{\sqrt{k_3}(\xi_3 - \eta_3)}{1 - k_3} \dots \frac{\sqrt{k_g}(\xi_g - \eta_g)}{1 - k_g} \right| \right\}. \quad (48)$$

Here, we have used the fact that in the parent universe $\lim_{T \rightarrow 0} \text{TAdS}_3$, the cosmological constant is equal to $V(\phi_2)$ (outside the bubble). Equation (48) indicates that the tunneling action B_{out} is a $(6g - 8)$ -variate function in the Schottky space.

To sum up, in this section, we generalize the tunneling action to the case where there are genus fluctuations. The main contribution comes from the third class of genus fluctuations, which does not affect the vacuum decay seed B_{seed} . Equations (30),

(31) and (32) indicate that the vacuum decay seed B_{seed} can be expressed as

$$B_{seed} = 4\pi \left\{ V^{-\frac{1}{2}}(\phi_2) \arcsin(\bar{\rho}\sqrt{V(\phi_2)}) - V^{-\frac{1}{2}}(\phi_1) \arcsin(\bar{\rho}\sqrt{V(\phi_1)}) \right. \\ \left. + \bar{\rho}\sqrt{1 - \bar{\rho}^2 V(\phi_2)} - \bar{\rho}\sqrt{1 - \bar{\rho}^2 V(\phi_1)} + \bar{\rho}^2 \int_{\phi_1}^{\phi_2} d\phi \sqrt{2(V(\phi) - V(\phi_2))} \right\}. \quad (49)$$

The relationship between the total tunneling action B and the vacuum decay seed B_{seed} is given by $B = B_{seed} + B_{out}$. If there are no genus fluctuations, $B_{out} = 0$, and all information of the vacuum decay dynamics is determined by the vacuum decay seed. In the case where there are genus fluctuations, B_{out} is described by equation (48). Taking $\partial B / \partial \bar{\rho} = 0$, one can obtain the bubble radius

$$\bar{\rho} = \frac{2\mu}{\sqrt{\mu^4 + \epsilon^2 + 2\mu^2(2V(\phi_2) + \epsilon)}}. \quad (50)$$

Equation (50) indicates that the radius $\bar{\rho}$ is determined by the tension of the domain wall and the energy density of the vacuum states.

3.2 Representing the tunneling action in the Siegel upper half space

The parameters $(\eta_2, k_2, \xi_3, \eta_3, k_3, \dots, \xi_g, \eta_g, k_g)$ in equation (48) specify the genus fluctuation. To include the contributions of all genus fluctuations (the third class), one needs to integrate over these parameters. However, the Schottky space is not simply connected, and different points in the Schottky space may correspond to the same genus fluctuations. Thus, it is not convenient to define the integral domain in the Schottky space. We will perform the summation of the genus fluctuations in the Siegel upper half space.

Using the relationship between the elements of the period matrix and the parameters (ξ_i, η_i, k_i) , one can transform the tunneling action from the Schottky space to the Siegel upper half space. Combining the normalized condition $(\xi_1 = 0, \xi_2 = 1, \eta_1 = \infty)$ of the Schottky group and equation (18), one can obtain

$$\eta_2 = \exp(-2\pi i \Pi(g)_{12}), \quad (51)$$

$$\xi_j = \eta_j \exp(2\pi i \Pi(g)_{1j}), \quad (52)$$

and

$$2\pi i \Pi(g)_{2j} = \ln \frac{(\eta_2 - \eta_j)(1 - \xi_j)}{(\eta_2 - \xi_j)(1 - \eta_j)}. \quad (53)$$

Substituting equations (51) and (52) into (53), one can obtain the relationship between the repelling fixed point η_j and the elements of the period matrix as

$$\eta_j = \frac{-\Delta_{2j} \pm \sqrt{\Delta_{2j}^2 - 4\Delta_{1j}\Delta_{3j}}}{2\Delta_{1j}}. \quad (54)$$

Here, the symbol “ \pm ” corresponds to two different results. In the later, we will show that only one of the results is meaningful in our model. The symbols Δ_{1j} , Δ_{2j} and Δ_{3j} are defined as

$$\Delta_{1j} \equiv \exp(2\pi i \Pi(g)_{2j}) - \exp(2\pi i \Pi(g)_{1j}), \quad (55)$$

$$\begin{aligned} \Delta_{2j} \equiv & 1 - \exp(2\pi i \Pi(g)_{2j}) \exp(-2\pi i \Pi(g)_{12}) - \exp(2\pi i \Pi(g)_{1j}) \exp(2\pi i \Pi(g)_{2j}) \\ & + \exp(-2\pi i \Pi(g)_{12}) \exp(2\pi i \Pi(g)_{1j}), \end{aligned} \quad (56)$$

$$\Delta_{3j} \equiv \exp(2\pi i \Pi(g)_{2j}) \exp(-2\pi i \Pi(g)_{12}) - \exp(-2\pi i \Pi(g)_{12}). \quad (57)$$

Equation (54) is the representation of the repelling fixed point η_j in the space $\mathbf{Sie}(g)$.

Equation (17) indicates that $k_i = \exp(2\pi i \Pi(g)_{ii})$. Using this result and incorporating equations (52) and (54) into equation (48), the tunneling action B_{out} becomes

$$\begin{aligned} B_{out} = & \frac{-4\pi}{\sqrt{-V(\phi_2)}} \left\{ \sum_{j=2}^g \ln \left| \frac{\exp(\pi i \Pi(g)_{jj})(\exp(2\pi i \Pi(g)_{1j}) - 1)}{1 - \exp(2\pi i \Pi(g)_{jj})} \right| \right. \\ & \left. + \sum_{j=2}^g \ln \left| \frac{-\Delta_{2j} \pm \sqrt{\Delta_{2j}^2 - 4\Delta_{1j}\Delta_{3j}}}{2\Delta_{1j}} \right| \right\}. \end{aligned} \quad (58)$$

Equations (54)-(58) show that in the space $\mathbf{Sie}(g)$, the tunneling action B_{out} is dependent on the set of parameters $(\Pi(g)_{22}, \Pi(g)_{33}, \dots, \Pi(g)_{gg}; \Pi(g)_{12}, \Pi(g)_{13}, \dots, \Pi(g)_{1g}; \Pi(g)_{23}, \Pi(g)_{24}, \dots, \Pi(g)_{2g})$. These parameters specify the genus fluctuations.

In our setup, the generator L_1 of the Schottky group $\mathbf{Sch}(L_1, L_2, \dots, L_g)$, the multiplier k_1 and the parameter $\Pi(g)_{11}$ ($2\pi i \Pi(g)_{11} = \ln k_1$) all correspond to the parent universe $\lim_{T \rightarrow 0} \text{TAdS}_3$. Other generators L_i ($i \neq 1$) correspond to the wormhole. Thus in equation (58), $j \geq 2$. The maximum value of j being g implies that the genus produced by the genus fluctuations is $g - 1$. The elements $\Pi(g)_{1j}$ ($j \neq 1$) should be interpreted

as the interaction between the parent universe $\lim_{T \rightarrow 0} \text{TAdS}_3$ and the wormhole j . And the elements $\Pi(g)_{ij}$ ($i, j \neq 1; i \neq j$) should be interpreted as the interaction between the wormhole i and j .

The tunneling action B_{out} in equation (58) is complicated. We need to simplify it. Defining $\mathcal{E}_j \equiv \xi_j - \eta_j$, then equation (18) implies that the element $\Pi(g)_{2j}$ can be expressed as

$$\Pi(g)_{2j} = \frac{1}{2\pi i} \ln \left(1 + \frac{\mathcal{E}_j}{\eta_2 - \xi_j} + \frac{\mathcal{E}_j}{\eta_j - \xi_2} - \frac{\mathcal{E}_j^2}{(\eta_2 - \xi_j)(\xi_2 - \eta_j)} \right). \quad (59)$$

Under the dilute wormhole gas approximation, the size of the wormhole is significantly smaller than their distance (equation (16)). Thus, equation (59) can be approximated as

$$\Pi(g)_{2j} \approx \frac{1}{2\pi i} \left(\frac{\mathcal{E}_j}{\eta_2 - \xi_j} + \frac{\mathcal{E}_j}{\eta_j - \xi_2} \right). \quad (60)$$

Equation (60) indicates that under the dilute wormhole gas approximation, the element $\Pi(g)_{2j}$ is small.

However, the element $\Pi(g)_{1j}$ represents the interaction between the parent universe and the wormhole. The dilute wormhole gas approximation does not imply that $\Pi(g)_{1j}$ is small. Therefore, according to equations (55)-(57), the quantities Δ_{1j} , Δ_{2j} and Δ_{3j} can be approximated as follows:

$$\Delta_{1j} \approx 1 - \exp(2\pi i \Pi(g)_{1j}), \quad \Delta_{3j} \approx 0, \quad (61)$$

$$\Delta_{2j} \approx (1 - \exp(2\pi i \Pi(g)_{1j})) (1 - \exp(-2\pi i \Pi(g)_{12})). \quad (62)$$

Equations (61) and (62) imply that the interactions between different wormholes are neglected, while the interactions between the parent universe and the wormholes are retained.

Substituting equations (61) and (62) into equation (58), one can obtain $B_{out} = \infty$ or

$$B_{out} = \frac{-4\pi}{\sqrt{-V(\phi_2)}} \left\{ \sum_{j=2}^g \ln \left| \frac{\exp(\pi i \Pi(g)_{jj}) (\exp(2\pi i \Pi(g)_{1j}) - 1)}{1 - \exp(2\pi i \Pi(g)_{jj})} \right| + \sum_{j=2}^g \ln \left| (\exp(-2\pi i \Pi(g)_{12}) - 1) \right| \right\}. \quad (63)$$

The symbol “ \pm ” in equation (58) corresponds to two different tunneling actions B_{out} . $B_{out} = \infty$ corresponds to “+”. This result does not make physical sense, so we disregard it. Equation (63) corresponds to “-”.

It is useful to denote $\Pi(g) = X + iY$, where X and Y are real symmetric $g \times g$ matrices. Then, one can easily prove that

$$\begin{aligned} & \left| \frac{\exp(\pi i \Pi(g)_{jj})(\exp(2\pi i \Pi(g)_{1j}) - 1)}{1 - \exp(2\pi i \Pi(g)_{jj})} (\exp(-2\pi i \Pi(g)_{12}) - 1) \right| \\ &= \exp(-\pi Y_{jj}) \cdot \left(\exp(-4\pi Y_{jj}) - 2\cos(2\pi X_{jj})\exp(-2\pi Y_{jj}) + 1 \right)^{-\frac{1}{2}} \\ & \quad \times \left(\exp(-4\pi Y_{1j}) - 2\cos(2\pi X_{1j})\exp(-2\pi Y_{1j}) + 1 \right)^{\frac{1}{2}} \\ & \quad \times \left(\exp(4\pi Y_{12}) - 2\cos(2\pi X_{12})\exp(2\pi Y_{12}) + 1 \right)^{\frac{1}{2}}. \end{aligned} \quad (64)$$

For convenience, we define

$$\Xi(\phi_2) \equiv 2\pi \sqrt{\frac{-1}{V(\phi_2)}}. \quad (65)$$

Combining equations (63)-(65), one can show that

$$\begin{aligned} B_{out} &= -\Xi(\phi_2)(g-1)\ln\left(1 + \exp(4\pi Y_{12}) - 2\cos(2\pi X_{12})\exp(2\pi Y_{12})\right) \\ & \quad - \Xi(\phi_2) \sum_{j=2}^g \left\{ -2\pi Y_{jj} - \ln\left(1 + \exp(-4\pi Y_{jj}) - 2\cos(2\pi X_{jj})\exp(-2\pi Y_{jj})\right) \right. \\ & \quad \left. + \ln\left(1 + \exp(-4\pi Y_{1j}) - 2\cos(2\pi X_{1j})\exp(-2\pi Y_{1j})\right) \right\}. \end{aligned} \quad (66)$$

Equation (66) shows that under the dilute wormhole gas approximation, the tunneling action B_{out} is a function of the set of variables $(X_{22}, X_{33}, \dots, X_{gg}, Y_{22}, Y_{33}, \dots, Y_{gg}, X_{12}, X_{13}, \dots, X_{1g}, Y_{12}, Y_{13}, \dots, Y_{1g})$.

The tunneling action B_{out} in equation (66) is still complicated. We have demonstrated that under the dilute wormhole gas approximation, the interactions between different wormholes are very weak, giving the rational to disregard them. To further simplify equation (66), we consider the case where the interactions between the parent universe and the wormholes are also small. Specifically, we focus on this case where

$$\Pi(g)_{ij} \quad (i, j \neq 1; i \neq j) \ll \Pi(g)_{1j} \quad (j \neq 1) \ll 1. \quad (67)$$

That is, all non-diagonal elements of the period matrix are small, and the interactions between different wormholes are significantly smaller than those between the parent universe and the wormholes.

Under condition (67), it is reasonable to neglect the interactions between different wormholes and approximate the terms related to the interactions between the parent universe and the wormhole to the first order. Thus, $\cos(2\pi X_{1j}) \approx 1$ and $\exp(\pm 2\pi Y_{1j}) \approx 1 \pm 2\pi Y_{1j}$. In addition, when deriving equations (17) and (18), we have used the small k_j limit. In this limit, $1 - \exp(2\pi i \Pi(g)_{jj}) \approx 1$ (this approximation had been used by Lyons and Hawking in reference [37]). Using these results, equation (66) can be simplified to

$$B_{out} = 2\Xi(\phi_2) \sum_{j=2}^g \{ \pi Y_{jj} - \ln(2\pi Y_{1j}) \} - 2\Xi(\phi_2)(g-1)\ln(2\pi Y_{12}). \quad (68)$$

The element $\Pi_{1j}(j \neq 1)$ represents the interaction between the parent universe and the wormhole “ j ”. Equation (68) indicates that the tunneling action B_{out} is independent of the variable X_{1j} . Thus, under the condition (67), $Y_{1j}(j \neq 1)$ can be used to describe the coupling strength between the parent universe and the wormhole “ j ”. Equation (68) is the representation of the tunneling action B_{out} in the space $\mathbf{Sie}(g)$. Noted that the vacuum decay seed B_{seed} is independent of the elements of the period matrix. Therefore, by representing B_{out} in the space $\mathbf{Sie}(g)$, the total tunneling action B is also represented in the space $\mathbf{Sie}(g)$.

4 Integration for the non-equivalent genus fluctuations

In the Coleman-De Luccia theory, the vacuum decay rate $e^{-B_{seed}}$ corresponds to the scenarios without genus fluctuations. However, during the vacuum decay process, space-time can fluctuate to generate one or more genus. Various fluctuations correspond to different vacuum decay processes. To calculate the total vacuum decay rate, all possible vacuum decay processes must be taken into account. Different genus fluctuations are represented by different handlebodies. Thus, one needs to integrate over the non-equivalent handlebodies. The vacuum decay rate associated with a specific type of genus fluctuation is $e^{-(B_{seed}+B_{out})}$, where B_{out} is given by equation (68). Therefore, the

total vacuum decay rate should be

$$\Gamma_{tot} = e^{-B_{seed}} + \sum_{g=2}^{\infty} \int_{\mathfrak{F}(g)} e^{-(B_{seed}+B_{out})} d\sigma(g), \quad (69)$$

where $\mathfrak{F}(g)$ and $d\sigma(g)$ represent the integral domain and the integral measure, respectively.

In equation (69), the first term on the right hand side represents the vacuum decay rate in the scenario without genus fluctuations. The second term accounts for the contribution of the genus fluctuation. The lower limit of the parameter g is $g = 2$. The reason is that $g = 2$ represents that the genus produced by the genus fluctuations is one. The vacuum decay seed B_{seed} is given by equation (49). The total tunneling action $B_{seed} + B_{out}$ are determined by equations (49) and (68).

In the integral domain $\mathfrak{F}(g)$, each point represents a different handlebody spacetime. In other words, different point in $\mathfrak{F}(g)$ corresponds to different genus fluctuation. To elucidate the integral domain $\mathfrak{F}(g)$, it is crucial to note that in the space $\mathbf{Sie}(g)$, when two period matrices are associated by a modular transformation, they describe the conformally equivalent Riemann surface Σ_g . The modular transformation between two period matrices $\Pi(g)^{(a)}$ and $\Pi(g)^{(b)}$ is defined as [32]

$$\Pi(g)^{(a)} = \frac{A\Pi(g)^{(b)} + B}{C\Pi(g)^{(b)} + D}, \quad (70)$$

where A, B, C, D are $g \times g$ matrices. Any element of these matrices is an integer. These matrices must satisfy the conditions $AB^T = BA^T$, $CD^T = DC^T$ and $AD^T - BC^T = \mathbb{I}_g$ [22, 24], where \mathbb{I}_g represents the $g \times g$ identity matrix and M^T denotes the transpose of the matrix M .

All modular transformations compose the modular group $\text{Sp}(2g, \mathbb{Z})$. It has two generators [38]

$$G(g)^{(1)} = \begin{pmatrix} \mathbb{I}_g & S \\ 0 & \mathbb{I}_g \end{pmatrix}, \quad G(g)^{(2)} = \begin{pmatrix} 0 & \mathbb{I}_g \\ -\mathbb{I}_g & 0 \end{pmatrix}. \quad (71)$$

Here, S is an arbitrary $g \times g$ symmetric integral matrix. Every element of the modular group $\text{Sp}(2g, \mathbb{Z})$ can be generated by these two generators. Equations (70) and (71) show that the generator $G(g)^{(1)}$ acts on the period matrix $\Pi(g)$ as $\Pi(g) \rightarrow \Pi(g) + S$. And the generator $G(g)^{(2)}$ acts on $\Pi(g)$ as $\Pi(g) \rightarrow -\Pi(g)^{-1}$. Some researchers may claim

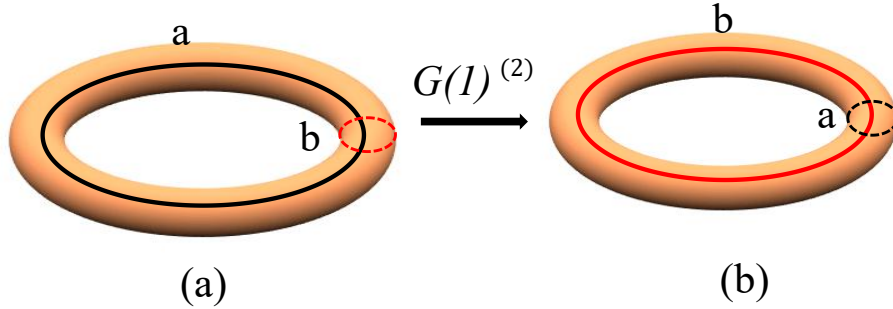


Figure 5: The transformation $G(1)^{(2)}$ transforms the torus (a) into the torus (b). In figure 5 (a) and (b), the tori have two dimensions a and b . The transformation $G(1)^{(2)}$ exchanges the two dimensions a and b .

that the modular group $\text{Sp}(2g, \mathbb{Z})$ has three generators [38, 39]. However, an additional generator can be generated by the generators $G(g)^{(1)}$ and $G(g)^{(2)}$ [38]. Therefore, it is enough to consider the generators $G(g)^{(1)}$ and $G(g)^{(2)}$.

The simplest case is the genus one closed Riemann surface Σ_1 . In this case, the period matrix $\Pi(1)$ is the modular parameter of the torus. The related modular group is $\text{Sp}(2, \mathbb{Z})$, which is generated by the following generators [50–52]

$$G(1)^{(1)} = \begin{pmatrix} 1 & 1 \\ 0 & 1 \end{pmatrix}, \quad G(1)^{(2)} = \begin{pmatrix} 0 & 1 \\ -1 & 0 \end{pmatrix}. \quad (72)$$

One can easily check that $G(1)^{(1)}$ and $G(1)^{(2)}$ satisfy the multiplication rules $(G(1)^{(2)})^2 = (G(1)^{(2)}G(1)^{(1)})^3 = \mathbb{I}_2$ [50]. The generator $G(1)^{(1)}$ generate the Dehn twist of the torus ($\Pi(1) \rightarrow \Pi(1) + 1$). The transformations generated by $G(1)^{(2)}$ exchange the two dimensions of the torus ($\Pi(1) \rightarrow -1/\Pi(1)$) [53], as shown in figure 5. If the torus $\Pi(1)$ represents a two dimensional spacetime, then the torus $-1/\Pi(1)$ also represents a two dimensional spacetime. Mathematically, the tori $\Pi(1)$ and $-1/\Pi(1)$ have the same conformal structure. However, physically, they represent different spacetimes as their time circles are different. Filling their interior will result in two non-equivalent three-dimensional handlebody spacetimes. Thus, the transformation $G(1)^{(2)}$ may alter the properties of the handlebody spacetime. A specific example is that the modular transformation $G(1)^{(2)}$ converts the TAdS₃ spacetime into the BTZ black hole [18].

The initial state (or final state) defined in the TAdS₃ spacetime and the BTZ black hole is a space slice. The space slice of the TAdS₃ spacetime is topologically non-equivalent to the space slice of the BTZ black hole. This indicates that one can not

define the same initial state (or final state) in the TAdS₃ spacetime and the BTZ black hole. At least, the topological structures of the initial states (or final states) defined in these two types of spacetimes are different. More generally, if the modular transformation $G(1)^{(2)}$ exchanges the time and space dimensions of the handlebody spacetime, then one can not define the same initial state (or final state) in these spacetimes associated by the transformation $G(1)^{(2)}$. Therefore, specifying the initial state implies that one has chosen a specific spacetime in the set of spacetimes which is associated by the modular transformation $G(1)^{(2)}$.

The generators $G(g)^{(1)}$ and $G(g)^{(2)}$ are the generalizations of the generators $G(1)^{(1)}$ and $G(1)^{(2)}$, respectively. Similar to the case of $G(1)^{(2)}$, one can easily show that $(G(g)^{(2)})^2 = \mathbb{I}_{2g}$. This implies that the modular transformations generated by $G(g)^{(2)}$ act on a genus g handlebody spacetime can only lead to another one different spacetime. The $G(g)^{(2)}$ acts on the period matrix as $\Pi(g) \rightarrow -\Pi(g)^{-1}$.

Under condition (67), the period matrix $\Pi(g)$ can be written as $\Pi(g) = \bigoplus_{i=1}^g \Pi(g)_{ii} + o(\Pi(g)_{ij})$, where $o(\Pi(g)_{ij})$ is a small term determined by the non-diagonal elements of Π . Utilizing the formula [54]

$$(A - B)^{-1} = A^{-1} + A^{-1}BA^{-1} + A^{-1}BA^{-1}BA^{-1} + \dots \quad (73)$$

one can express the period matrix $-\Pi(g)^{-1}$ as

$$\begin{aligned} -\Pi(g)^{-1} = & - \left(\bigoplus_{i=1}^g \Pi(g)_{ii}^{-1} \right) \left\{ \mathbb{I}_g - o(\Pi(g)_{ij}) \left(\bigoplus_{i=1}^g \Pi(g)_{ii}^{-1} \right) \right. \\ & \left. + o(\Pi(g)_{ij}) \left(\bigoplus_{i=1}^g \Pi(g)_{ii}^{-1} \right) o(\Pi(g)_{ij}) \left(\bigoplus_{i=1}^g \Pi(g)_{ii}^{-1} \right) + \dots \right\}. \end{aligned} \quad (74)$$

The predominant term on the right hand side of equation (74) is $-\bigoplus_{i=1}^g \Pi(g)_{ii}^{-1}$.

The dominant terms of $\Pi(g)$ and $-\Pi(g)^{-1}$ are $\bigoplus_{i=1}^g \Pi(g)_{ii}$ and $-\bigoplus_{i=1}^g \Pi(g)_{ii}^{-1}$, respectively. Both $\bigoplus_{i=1}^g \Pi(g)_{ii}$ and $-\bigoplus_{i=1}^g \Pi(g)_{ii}^{-1}$ represent multiple disconnected spacetimes. We have demonstrated that it is impossible to define the same initial state (or final state) in the spacetimes $\Pi(g)_{ii}$ and $-\Pi(g)_{ii}^{-1}$. Thus, One also can not define the same initial state (or final state) in the spacetimes $\bigoplus_{i=1}^g \Pi(g)_{ii}$ and $-\bigoplus_{i=1}^g \Pi(g)_{ii}^{-1}$. Therefore, it

is reasonable to infer that one can not define the same initial state (or final state) in the handlebody spacetimes $\Pi(g)$ and $-\Pi(g)^{-1}$. In our model, the initial state is specified. It is the space slice $\tau_E = -\infty$ of the parent universe $\lim_{T \rightarrow 0} \text{TAdS}_3$. Assuming that this initial state can be defined in the spacetime $\Pi(g)$, then in the spacetime $-\Pi(g)^{-1}$, one can not define the same initial state. Therefore, the spacetime $-\Pi(g)^{-1}$ should not be included in the integral domain $\mathfrak{F}(g)$. Consequently, specifying the initial state breaks down the modular symmetry $\text{Sp}(2g, \mathbb{Z})$.

We denote the group freely generated by the generator $G(g)^{(1)}$ as \mathbf{P} . The group \mathbf{P} is a subgroup of $\text{Sp}(2g, \mathbb{Z})$. One can easily verify that the modular transformations in the group \mathbf{P} act trivially on the tunneling action B_{out} and the vacuum decay seed B_{seed} . Therefore, in our model, the spacetimes associated by the modular transformations in the group \mathbf{P} are physically equivalent. In the studies of the partition function of the high genus AdS_3 spacetime, other researchers also suggested that the spacetimes associated by the group \mathbf{P} are equivalent [10, 22, 24, 55]. Taking the above arguments into consideration, when summarizing over different genus fluctuations, one does not need to consider the spacetimes associated by the modular transformations which are generated by $G(g)^{(1)}$ and $G(g)^{(2)}$. Any element of the modular group $\text{Sp}(2g, \mathbb{Z})$ can be generated by $G(g)^{(1)}$ and $G(g)^{(2)}$. Therefore, any modular transformation in the modular group $\text{Sp}(2g, \mathbb{Z})$ does not need to be considered.

The fundamental domain of the modular group $\text{Sp}(2g, \mathbb{Z})$ in the space $\mathbf{Sie}(g)$ can be expressed as $\mathbf{Sie}(g)/\text{Sp}(2g, \mathbb{Z})$. Any point in $\mathbf{Sie}(g)/\text{Sp}(2g, \mathbb{Z})$ can not be associated by the transformations in the modular group $\text{Sp}(2g, \mathbb{Z})$. And any point in the space $\mathbf{Sie}(g)$ can be associated with one point in $\mathbf{Sie}(g)/\text{Sp}(2g, \mathbb{Z})$. The fundamental domain $\mathbf{Sie}(g)/\text{Sp}(2g, \mathbb{Z})$ is a connected subspace of the space $\mathbf{Sie}(g)$. Any period matrix outside the fundamental domain $\mathbf{Sie}(g)/\text{Sp}(2g, \mathbb{Z})$ can always be associated with only one period matrix inside the fundamental domain $\mathbf{Sie}(g)/\text{Sp}(2g, \mathbb{Z})$. Thus, when summing different genus fluctuations, one does not need to consider the period matrix outside the fundamental domain $\mathbf{Sie}(g)/\text{Sp}(2g, \mathbb{Z})$. In other words, the spacetimes outside the fundamental domain $\mathbf{Sie}(g)/\text{Sp}(2g, \mathbb{Z})$ should not be included in the integral domain $\mathfrak{F}(g)$. The handlebodies in the fundamental domain $\mathbf{Sie}(g)/\text{Sp}(2g, \mathbb{Z})$ that do not satisfy condition (67) should also not be included in the integral domain $\mathfrak{F}(g)$. Therefore,

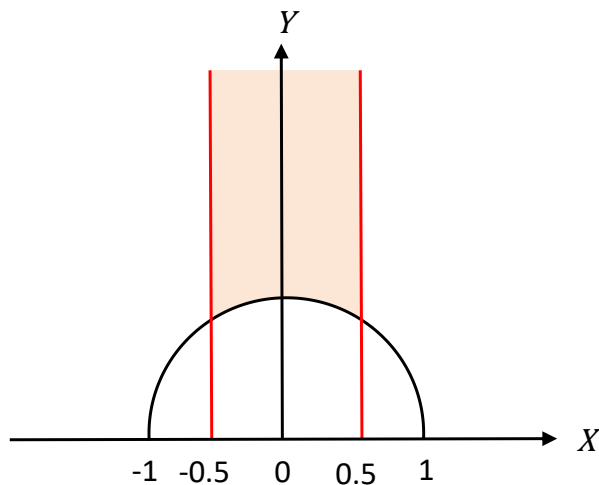


Figure 6: The fundamental domain of the modular group $\text{Sp}(2, \mathbb{Z})$ in the Siegel upper half space $\mathbf{Sie}(1)$. The shadow represents the fundamental domain $\mathbf{Sie}(1)/\text{Sp}(2, \mathbb{Z})$. X and Y represent the real part and the imaginary part of the period matrix $\Pi(1)$, respectively. The equations of the red lines are $X = \pm 0.5$. And the equation of the black curve is $X^2 + Y^2 = 1$ with $Y > 0$. The intersections of the black curve and the red lines are $(\pm 0.5, \frac{\sqrt{3}}{2})$.

the integral domain $\mathfrak{F}(g)$ is a subspace of the fundamental domain $\mathbf{Sie}(g)/\text{Sp}(2g, \mathbb{Z})$.

It is well known that the fundamental domain of the modular group $\text{Sp}(2, \mathbb{Z})$ in the space $\mathbf{Sie}(1)$ is determined by the equation [56]

$$\mathbf{Sie}(1)/\text{Sp}(2, \mathbb{Z}) = \left\{ \begin{array}{l} |\Pi(1)| \geq 1 \\ |X| = |\text{Re}(\Pi(1))| \leq \frac{1}{2} \end{array} \right. . \quad (75)$$

Here, $\text{Re}(\Pi(1))$ represents the real part of the period matrix $\Pi(1)$. The shadow in figure 6 represents the fundamental domain $\mathbf{Sie}(1)/\text{Sp}(2, \mathbb{Z})$. It is a two dimensional connected space. No two points in the shadow (excluding the points on the boundaries) can be associated by the modular transformation in the group $\text{Sp}(2, \mathbb{Z})$. Thus, various points in the shadow correspond to various handlebody spacetimes. And every point in the shadow adheres to equation (75). The boundaries of the fundamental domain $\mathbf{Sie}(1)/\text{Sp}(2, \mathbb{Z})$ are defined by the equations $X = \pm 0.5$ and $X^2 + Y^2 = 1$ with $Y > 0$.

In the case where the genus fluctuations only produce one genus, the period matrix is

$$\Pi(2) = \begin{pmatrix} \Pi(2)_{11} & \Pi(2)_{12} \\ \Pi(2)_{21} & \Pi(2)_{22} \end{pmatrix}. \quad (76)$$

Here, $\Pi(2)_{11}$ and $\Pi(2)_{22}$ correspond to the parent universe $\lim_{T \rightarrow 0} \text{TAdS}_3$ and the wormhole, respectively. $\Pi(2)_{12} = \Pi(2)_{21}$ represents the interaction between the parent universe

and the wormhole. The temperature of the parent universe is zero implies that $\Pi(2)_{11} = \infty$. When the interaction $\Pi(2)_{12} = 0$, $\Pi(2) = \Pi(2)_{11} \oplus \Pi(2)_{22}$, indicating that the parent universe and the wormhole is disconnected. The wormhole degenerates into a genus one universe (a solid torus). Various points in the shadow of figure 6 represent different genus one universes.

When there is a small interaction between the parent universe and the wormhole, the period matrix (76) can be expressed as $\Pi(2) = \Pi(2)_{11} \oplus \Pi(2)_{22} + o(\Pi(2)_{12})$. Here, $o(\Pi(2)_{12})$ is a small term determined by the interaction $\Pi_{12}(2)$. The predominant part of the period matrix $\Pi(2)$ is $\Pi(2)_{11} \oplus \Pi(2)_{22}$. Since the interaction is small, its impact on the features of the period matrix $\Pi(2)$ is small. Therefore, it can be anticipated that within the fundamental domain $\mathbf{Sie}(2)/\mathrm{Sp}(4, \mathbb{Z})$, the value range of the parameter $\Pi(2)_{22}$ can be expressed as

$$\begin{cases} |\Pi(2)_{22}| \geq 1 + \delta_1 \\ |\mathrm{Re}(\Pi(2)_{22})| \leq \frac{1}{2} + \delta_2 \end{cases} \quad (77)$$

Here, δ_1 and δ_2 represent the influence of the interaction $\Pi(2)_{12}$. For any genus g , the fundamental domain $\mathbf{Sie}(g)/\mathrm{Sp}(2g, \mathbb{Z})$ always fulfills the condition $|X_{ij}| \leq \frac{1}{2}$ [38]. This indicates that $\delta_2 = 0$. Since $o(\Pi(2)_{12})$ is small, one can expect that δ_1 is also small. Therefore, equation (75) can still be used approximately to represent the value range of the parameter $\Pi(2)_{22}$ in the fundamental domain $\mathbf{Sie}(2)/\mathrm{Sp}(4, \mathbb{Z})$.

A small $\Pi(2)_{12}$ implies that both X_{12} and Y_{12} are small. Denoting the upper limit of X_{12} and Y_{12} as α and β (meaning that if $X_{12} > \alpha$ or $Y_{12} > \beta$, condition (67) will break down), respectively. Then the value range of X_{12} and Y_{12} are $|X_{12}| < \alpha$ ($\alpha > 0$) and $0 \leq Y_{12} \leq \beta$, respectively. Without the restriction of condition (67), $\alpha = \frac{1}{2}$ [38]. The minimum value of Y_{12} being greater than zero is because the imaginary part of any element in the space $\mathbf{Sie}(g)$ is non-negative. For convenience, we define $\mathfrak{D} \equiv \{(x, y) \mid -\alpha < x < \alpha; 0 \leq y \leq \beta\}$. Considering the above conclusions, when $\Pi(2)_{12}$ is small, the integral domain $\mathfrak{F}(2)$ should be selected as $\mathfrak{F}(2) = (\mathbf{Sie}(1)/\mathrm{Sp}(2, \mathbb{Z})) \otimes \mathfrak{D}$. Points in $\mathbf{Sie}(1)/\mathrm{Sp}(2, \mathbb{Z})$ represent various wormholes, while points in \mathfrak{D} represent different coupling between the wormhole and the parent universe.

Under the dilute wormhole gas approximation, different wormholes are independent of each other. Each wormhole corresponds to an integral domain $\mathfrak{F}(2)$. Therefore, the

integral domain $\mathfrak{F}(g)$ should be

$$\mathfrak{F}(g) = \bigotimes_{j=2}^g \mathfrak{F}(2) = \bigotimes_{j=2}^g \left((\mathbf{Sie}(1)/\mathrm{Sp}(2, \mathbb{Z})) \otimes \mathfrak{D} \right). \quad (78)$$

Combining equations (75) and (78), one can show that equation (78) can be written as

$$\mathfrak{F}(g) = \left\{ \begin{array}{l} |X_{jj}| \leq \frac{1}{2} \\ Y_{jj} \geq (1 - X_{jj}^2)^{\frac{1}{2}} \\ |X_{1j}| \leq \alpha \\ 0 \leq Y_{1j} \leq \beta \end{array} \right., \quad j = 2, 3, \dots, g. \quad (79)$$

The parameters α and β are subject to two conditions. The first condition is that equation (67) must not be violated. The second condition is that the integral domain $\mathfrak{F}(g)$ must be a subspace of the fundamental domain $\mathbf{Sie}(g)/\mathrm{Sp}(2g, \mathbb{Z})$.

Equation (79) is derived under condition (67). Utilizing equations (17) and (67), one can show that

$$|k_j| = \exp(-2\pi Y_{jj}) \leq 0.0043. \quad (80)$$

Hence, under condition (67), it is sufficient to approximate the Schottky group $\mathbf{Sch}(L_1, L_2, \dots, L_g)$ to the first order of the multiplier k_j .

For the integral measure $d\sigma(g)$, equation (79) implies that the integral variables are $(X_{22}, X_{33}, \dots, X_{gg}, Y_{22}, Y_{33}, \dots, Y_{gg}, X_{12}, X_{13}, \dots, X_{1g}, Y_{12}, Y_{13}, \dots, Y_{1g})$. Thus, the most general form of $d\sigma(g)$ is

$$\begin{aligned} d\sigma(g) = & \mathfrak{G}(X_{22}, \dots, Y_{1g}) dX_{22} dX_{33} \cdots dX_{gg} dY_{22} dY_{33} \cdots dY_{gg} \\ & \times dX_{12} dX_{13} \cdots dX_{1g} dY_{12} dY_{13} \cdots dY_{1g}. \end{aligned} \quad (81)$$

Here, $\mathfrak{G}(X_{22}, \dots, Y_{1g})$ represents the determinant of the metric defined in the space $(X_{22}, X_{33}, \dots, X_{gg}, Y_{22}, Y_{33}, \dots, Y_{gg}, X_{12}, X_{13}, \dots, X_{1g}, Y_{12}, Y_{13}, \dots, Y_{1g})$.

In the space $\mathbf{Sie}(g)$, the modular invariant uniquely determines the integral measure up to a constant factor [38]. However, our model lacks the modular invariant. Thus, one cannot determine the function $\mathfrak{G}(X_{22}, \dots, Y_{1g})$ based on the modular symmetry. The path integral typically corresponds to the Lebesgue measure in the configuration space. Following this reasoning, one may consider setting $\mathfrak{G}(X_{22}, \dots, Y_{1g}) = 1$. As a result, the integral measure (81) becomes

$$\begin{aligned} d\sigma(g) = & dX_{22} dX_{33} \cdots dX_{gg} dY_{22} dY_{33} \cdots dY_{gg} \\ & \times dX_{12} dX_{13} \cdots dX_{1g} dY_{12} dY_{13} \cdots dY_{1g}. \end{aligned} \quad (82)$$

Equation (82) implies that different handlebodies correspond to the same amplitude in the real-time path integral.

Equation (81) or (82) shows that the dimension of the integral space $(X_{22}, X_{33}, \dots, X_{gg}, Y_{22}, Y_{33}, \dots, Y_{gg}, X_{12}, X_{13}, \dots, X_{1g}, Y_{12}, Y_{13}, \dots, Y_{1g})$ is $4g - 4$. Thus, the dimension of the integral space differs from that of the dimension of the Schottky space and the Teichmüller space of the Riemann surface Σ_g . This result arises from two main reasons. Firstly, we only focus on genus fluctuations that adhere to condition (67). Any other spacetime configurations not meeting this criterion are outside the scope of this study. Secondly, the parameters X_{11} and Y_{11} are associated with the parent universe. When summing over the genus fluctuations, these parameters should not serve as integral variables.

We pointed out that without restricting the interactions between the parent universe and the wormholes to be small, equations (55)-(58) indicate that the tunneling action B_{out} becomes a function of the variables $(X_{22}, X_{33}, \dots, X_{gg}, Y_{22}, Y_{33}, \dots, Y_{gg}, X_{12}, X_{13}, \dots, X_{1g}, Y_{12}, Y_{13}, \dots, Y_{1g}, X_{23}, X_{24}, \dots, X_{2g}, Y_{23}, Y_{24}, \dots, Y_{2g})$. In such a scenario, the dimension of the integral space equals $6g - 8$. Thus, after subtracting the dimensions related to the multiplier k_1 , the dimension of the Schottky space of the Riemann surface Σ_g aligns with that of the integral space.

To sum up, we show that specifying the initial state will break down the modular symmetry of the model. The integral domain $\mathfrak{F}(g)$ is a subspace of the fundamental domain $\mathbf{Sie}(g)/\mathrm{Sp}(2g, \mathbb{Z})$. Under condition (67), the integral domain $\mathfrak{F}(g)$ can be selected as (79). Using equations (69), (79) and (82), one can complete the summation over the physically non-equivalent genus fluctuations. Although the parameters α and β in equation (79) are unspecified, we will show that their precise values are not important for the qualitative results.

5 The tunneling rate

5.1 Genus creation rate

Generally, up to the leading order of the WKB approximation, the quantum tunneling rate is equal to the tunneling probability [57–59]. Thus, in the semiclassical region, the

tunneling rate from the initial state $|i\rangle$ to the final state $|f\rangle$ is given by

$$\exp\{-2(S_E(|i\rangle \rightarrow |f\rangle) - S_E(|i\rangle))\}. \quad (83)$$

Here, $S_E(|i\rangle \rightarrow |f\rangle)$ represents the Euclidean action of the instanton trajectory $|i\rangle \rightarrow |f\rangle$. The instanton trajectory is the solution of the Euclidean Euler-Lagrange dynamical equation. And $S_E(|i\rangle)$ represents the Euclidean action of the process in which the system remains in the initial state $|i\rangle$. One can check that in the Coleman-De Luccia theory, the factor $e^{-B_{seed}}$ exhibits a similar structure to equation (83).

Comparing equations (34), (35), (41) and (83), it can be observed that the factor $e^{-B_{out}}$ has a similar structure to equation (83). The factor $\lim_{T \rightarrow 0} V(\phi_2, T) Rvol_T(g = n + 1)$ in equation (41) represents the regularized Euclidean action of the process in which the genus fluctuations produce $g - 1$ genus. Therefore, the factor $e^{-B_{out}}$ should be interpreted as the rate to create the genus $g - 1$ configuration $(\Pi(g)_{22}, \Pi(g)_{33}, \dots, \Pi(g)_{gg}, \Pi(g)_{12}, \Pi(g)_{13}, \dots, \Pi(g)_{1g})$. Consequently, the total tunneling rate from the genus zero AdS_3 state to the genus $g - 1$ AdS_3 state is

$$\Gamma(g - 1) = \int_{\mathfrak{F}(g)} e^{-B_{out}} d\sigma(g). \quad (84)$$

The integral domain $\mathfrak{F}(g)$ and the tunneling action B_{out} are given by equations (79) and (68), respectively. The integral measure $d\sigma(g)$ is given by equation (82).

In our model, $\Pi(2)_{11} = \infty$. Thus, the genus one spacetime can be parameterized by the parameters $(\Pi(2)_{22}, \Pi(2)_{12})$. This type of spacetime represents a fluctuation process of a wormhole. Setting $g = 2$ in equation (68), one can obtain that the rate of creating the genus $(\Pi(2)_{22}, \Pi(2)_{12})$ is

$$\Gamma(\Pi(2)_{22}, \Pi(2)_{12}) = \exp\{-2\pi\Xi(\phi_2)Y_{22}\}(2\pi Y_{12})^{4\Xi(\phi_2)}. \quad (85)$$

Equation (85) shows that the rate $\Gamma(\Pi(2)_{22}, \Pi(2)_{12})$ relies on the parameters $V(\phi_2)$, Y_{22} and Y_{12} . $V(\phi_2)$ is the cosmological constant. The parameter Y_{12} represents the coupling strength between the parent universe and the wormhole.

In order to illustrate the meaning of the parameter Y_{22} , we consider the limit as Y_{12} approaches zero. In this scenario, the wormhole becomes a torus $\Pi(2)_{22}$ and is disconnected from the parent universe. One can use the lattice $L(1, \Pi(2)_{22}) \equiv \{m + n\Pi(2)_{22} \mid$

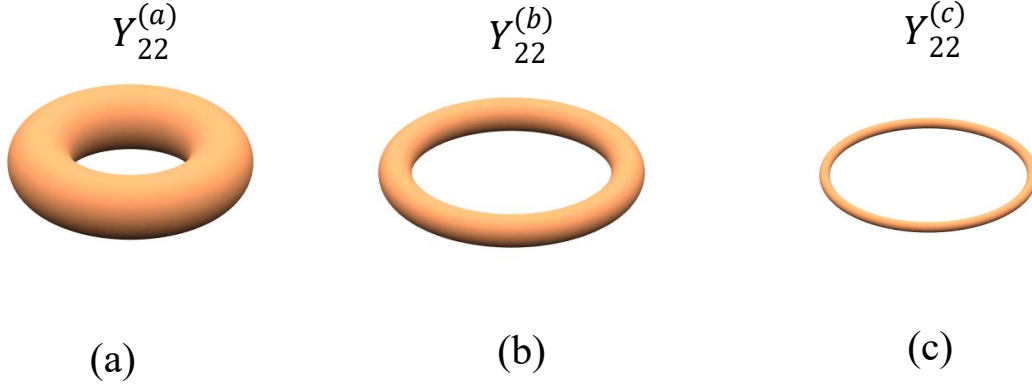


Figure 7: Three conformal nonequivalent tori. The parameters $Y_{22}^{(a)}$, $Y_{22}^{(b)}$, and $Y_{22}^{(c)}$ represent the imaginary part of the modular parameter of the torus (a), (b), and (c), respectively. We have set $Y_{22}^{(c)} > Y_{22}^{(b)} > Y_{22}^{(a)} > 1$. Torus (a) is fatter than torus (b), which in turn is fatter than torus (c).

$m, n \in \mathbb{Z}$ in the complex plane \mathbb{C} to represent the torus [53]. Connecting the points $(0, 0)$, $(1, 0)$, $(\text{Re}(\Pi(2)_{22}), \text{Im}(\Pi(2)_{22}))$, $(\text{Re}(\Pi(2)_{22}) + 1, \text{Im}(\Pi(2)_{22}))$, one can obtain a parallelogram in the complex plane. The base and the height of the parallelogram are 1 and $\text{Im}(\Pi(2)_{22}) = Y_{22}$, respectively. Roughly speaking, a smaller difference between the base and height of the parallelogram corresponds to a fatter torus. That is, the factor $|Y_{22} - 1|$ being smaller implies that the torus is fatter. $|Y_{22} - 1| = 0$ corresponds to the fattest torus. Equation (85) shows that the creation rate $\Gamma(\Pi(2)_{22}, \Pi_{12})$ is independent of the parameter X_{22} . For simplicity, we consider the case where $X_{22} = 0$. In this instance, equation (79) indicates that $Y_{22} \geq 1$. Thus, a smaller Y_{22} leads to a smaller $|Y_{22} - 1|$ and this corresponds to a fatter torus, as shown in figure 7. When $Y_{12} \neq 0$, this torus connects with the parent universe and becomes a wormhole. Therefore, a smaller Y_{22} corresponds to a fatter wormhole.

Figure 8 illustrates the variations in the genus creation rate $\Gamma(\Pi(2)_{22}, \Pi_{12})$. Figures 8 (a) and (c) show that a stronger coupling strength corresponds to a larger genus creation rate $\Gamma(\Pi(2)_{22}, \Pi_{12})$. Figures 8 (a) and (b) show that as the parameter Y_{22} increases, the genus creation rate $\Gamma(\Pi(2)_{22}, \Pi_{12})$ decreases. This indicates that a fatter wormhole is easier to create than a thin one in the parent universe $\lim_{T \rightarrow 0} \text{TAdS}_3$. Figures 8 (b) and (c) reveal that as the absolute value of the cosmological constant increases, the genus creation rate $\Gamma(\Pi(2)_{22}, \Pi_{12})$ also increases. That is, the genus fluctuations are more likely to occur in the AdS_3 spacetime with a more negative cosmological constant.

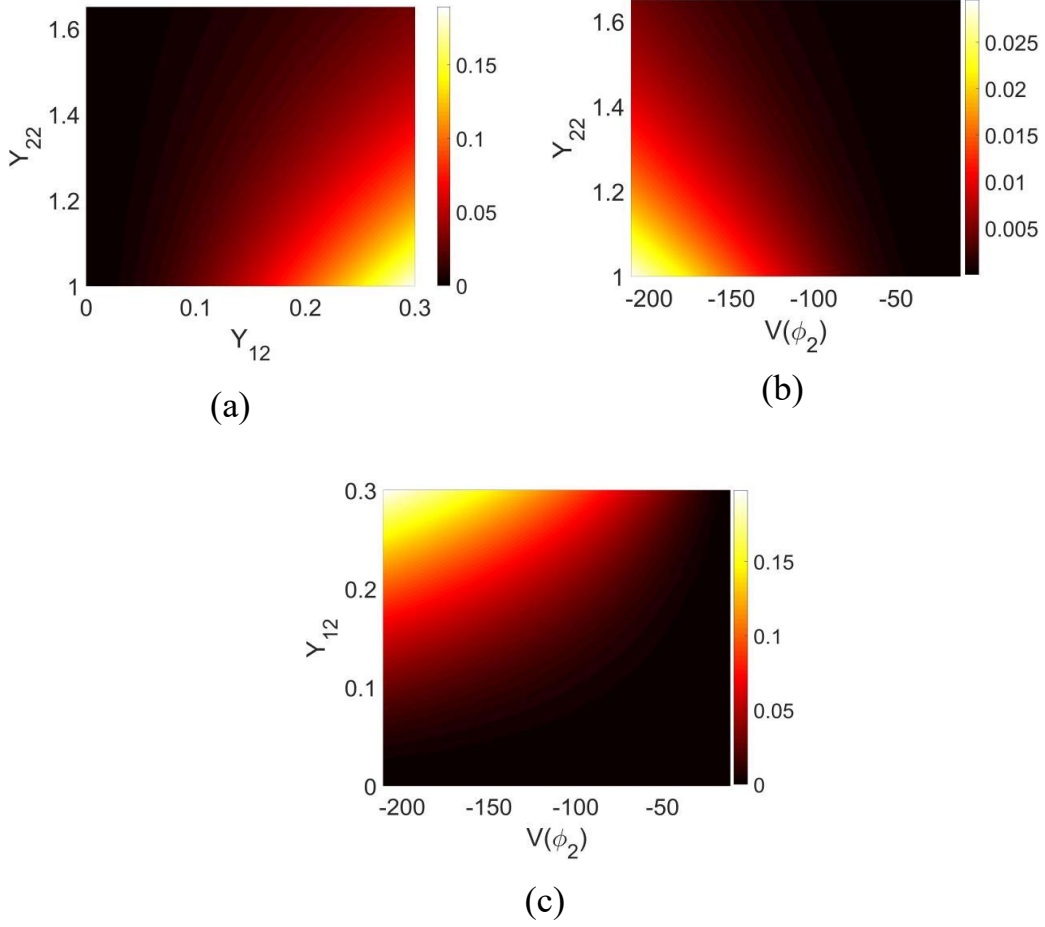


Figure 8: Variations in the Genus creation rate $\Gamma(\Pi(2)_{22}, \Pi_{12})$. In figures 8 (a) and (b), the vertical axes represent the parameter Y_{22} . In figures 8 (b) and (c), the horizontal axes represent the cosmological constant $V(\phi_2)$. The horizontal axis of figure 8 (a) and the vertical axis of figure 8 (b) represent the coupling strength Y_{12} . Different colors in figures 8 (a), (b) and (c) represent various values of the genus creation rate $\Gamma(\Pi(2)_{22}, \Pi_{12})$. The parameters are set as follows: in figure 8 (a), $V(\phi_2) = -200$; in figure 8 (b), $Y_{12} = 0.1$; in figure 8 (c), $Y_{22} = 1$.

For the high genus spacetime fluctuations, the tunneling rate from the genus zero spacetime state to the genus $g-1$ spacetime state is given by equation (84). Substituting equations (68), (79) and (82) into (84), the tunneling rate $\Gamma(g-1)$ can be written as

$$\begin{aligned} \Gamma(g-1) = & \int_{-\frac{1}{2}}^{\frac{1}{2}} dX_{22} \int_{-\frac{1}{2}}^{\frac{1}{2}} dX_{33} \cdots \int_{-\frac{1}{2}}^{\frac{1}{2}} dX_{gg} \int_{\sqrt{1-X_{22}^2}}^{\infty} dY_{22} \int_{\sqrt{1-X_{33}^2}}^{\infty} dY_{33} \cdots \int_{\sqrt{1-X_{gg}^2}}^{\infty} dY_{gg} \\ & \int_{-\alpha}^{\alpha} dX_{12} \int_{-\alpha}^{\alpha} dX_{13} \cdots \int_{-\alpha}^{\alpha} dX_{1g} \int_0^{\beta} dY_{12} \int_0^{\beta} dY_{13} \cdots \int_0^{\beta} dY_{1g} \\ & \times \prod_{j=2}^g \left(\exp\{-2\pi\Xi(\phi_2)Y_{jj}\} (2\pi Y_{12})^{2\Xi(\phi_2)} (2\pi Y_{1j})^{2\Xi(\phi_2)} \right). \end{aligned} \quad (86)$$

Using the approximation $\sqrt{1-X_{jj}^2} \approx 1 - \frac{1}{2}X_{jj}^2 + o(X_{jj}^4)$, one can complete the integration over the variables $(X_{22}, X_{33}, \dots, X_{gg}, Y_{22}, Y_{33}, \dots, Y_{gg}, X_{12}, X_{13}, \dots, X_{1g}, Y_{12}, Y_{13}, \dots, Y_{1g})$. Consequently, equation (86) becomes

$$\Gamma(g-1) = \frac{2\Xi(\phi_2) + 1}{2g\Xi(\phi_2) + 1} \left(\Theta(\phi_2) \operatorname{erfi}\left(\frac{1}{2}\sqrt{\pi\Xi(\phi_2)}\right) \right)^{g-1}, \quad (87)$$

where,

$$\Theta(\phi_2) \equiv 2\alpha \frac{\exp\{-2\pi\Xi(\phi_2)\}}{2\pi\Xi(\phi_2)} \frac{(2\pi)^{4\Xi(\phi_2)}}{2\Xi(\phi_2) + 1} \Xi(\phi_2)^{-\frac{1}{2}} \beta^{4\Xi(\phi_2)+1} \quad (88)$$

and

$$\operatorname{erfi}(x) \equiv \frac{2}{\sqrt{\pi}} \int_0^x e^{t^2} dt = \frac{2}{\sqrt{\pi}} \sum_{k=0}^{\infty} \frac{x^{2k+1}}{(2k+1)k!} \quad (89)$$

is the imaginary error function.

In equation (86), the factor

$$\prod_{j=2}^g \left(\exp\{-2\pi\Xi(\phi_2)Y_{jj}\} (2\pi Y_{12})^{2\Xi(\phi_2)} (2\pi Y_{1j})^{2\Xi(\phi_2)} \right) \quad (90)$$

is equal to $e^{-B_{out}}$. Thus, the factor (90) represents the tunneling probability from the parent universe $\lim_{T \rightarrow 0} \text{TAdS}_3$ to the genus $g-1$ configuration $(\Pi(g)_{22}, \Pi(g)_{33}, \dots, \Pi(g)_{gg}, \Pi(g)_{12}, \Pi(g)_{13}, \dots, \Pi(g)_{1g})$. Up to the leading order of the WKB approximation, it also denotes the tunneling rate.

Under the dilute wormhole gas approximation, the fluctuations of each genus are independent of each other. Thus, the factor (90) can be expressed as the multiplication

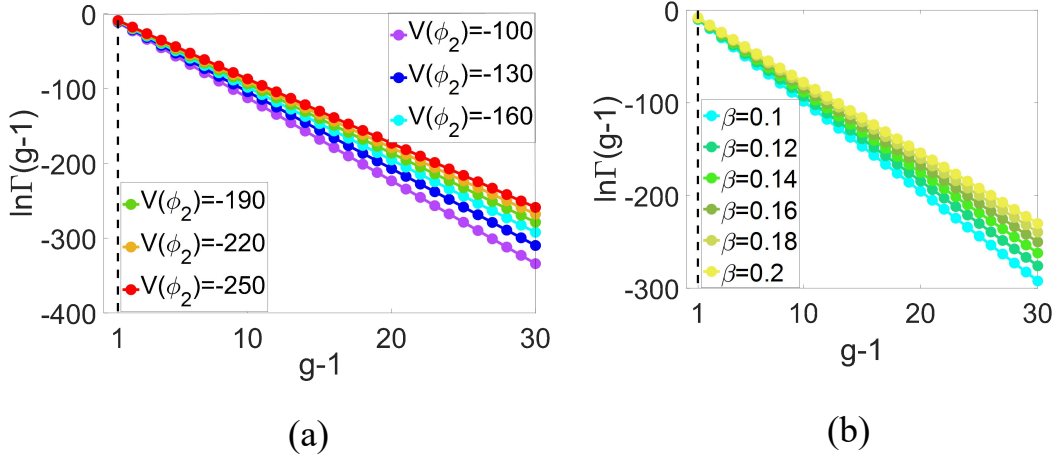


Figure 9: Variations in the tunneling rate $\Gamma(g-1)$ versus genus. In figures 9 (a) and (b), the horizontal axes represent the genus produced by the genus fluctuation. The vertical axes represent the logarithm of the tunneling rate $\Gamma(g-1)$. The parameters are set as follows: in figure 9 (a), $\alpha = \beta = 0.1$; in figure 9 (b), $\alpha = 0.1$ and $V(\phi_2) = -160$.

of the tunneling probabilities of each genus. To illustrate this, we temporarily rewritten $e^{-B_{out}}$ in the Schottky space. In the small k_j limit, utilizing equation (48), one can derive

$$e^{-B_{out}} = \prod_{j=2}^g |\sqrt{k_j}(\xi_j - \eta_j)|^{2\Xi(\phi_2)}. \quad (91)$$

It is easy to show that

$$|\sqrt{k_2}(\xi_2 - \eta_2)|^{2\Xi(\phi_2)} = \exp\{-2\pi\Xi(\phi_2)Y_{22}\}(2\pi Y_{12})^{4\Xi(\phi_2)}. \quad (92)$$

Comparing equations (92) and (85), one can find that $|\sqrt{k_2}(\xi_2 - \eta_2)|^{2\Xi(\phi_2)} = \Gamma(\Pi(2)_{22}, \Pi(2)_{12})$. This indicates that the factor $|\sqrt{k_2}(\xi_2 - \eta_2)|^{2\Xi(\phi_2)}$ signifies the tunneling probability of creating the genus $(\Pi(2)_{22}, \Pi(2)_{12})$. Therefore, the factor $|\sqrt{k_j}(\xi_j - \eta_j)|^{2\Xi(\phi_2)}$ represents the tunneling probability of creating the genus $(\Pi(2)_{jj}, \Pi(2)_{1j})$. Hence, the factor (90) indeed equals the product of the tunneling probability of each genus.

Figure 9 illustrates the variations in the tunneling rate $\Gamma(g-1)$. Both figures 9 (a) and (b) show that as the genus number increases, the tunneling rate $\Gamma(g-1)$ decreases rapidly, indicating that the dominant fluctuations are the one genus fluctuations. This result can be inferred from another perspective: under the dilute wormhole gas approximation, the fluctuations of different genus are independent of each other. The probability to create multiple genus can be viewed as the product of the probabili-

ties of producing each genus. Therefore, it is more difficult to produce a higher genus spacetime. This leads to a decrease in $\Gamma(g-1)$ with $g-1$.

Figure 9 (a) also reveals that in the AdS₃ spacetime with a more negative cosmological constant, the tunneling rate $\Gamma(g-1)$ is larger, which is consistent with the findings from figures 8 (b) and (c). Figure 9 (b) shows that the exact value of the parameter β has no impact on the qualitative result. In addition, equations (87) and (88) indicate that $\Gamma(g-1) \propto \alpha^{g-1}$. Therefore, the qualitative results obtained from figure 9 are also unaffected by the specific value of the parameter α .

To sum up, in this section, we demonstrate that the rate of creating the spacetime configuration $(\Pi(2)_{22}, \Pi_{12})$ should be described by the quantity $\Gamma(\Pi(2)_{22}, \Pi_{12})$. We show that the genus fluctuations is more likely to occur in the AdS₃ spacetime with a more negative cosmological constant. We also show that the fatter wormhole is easier to create than the thin wormhole. The total rate of tunneling from the genus zero AdS₃ state to the high genus spacetime state is described by $\Gamma(g-1)$. The rate $\Gamma(g-1)$ rapidly decreases as the genus increases. Thus, the dominant fluctuations are the genus one fluctuations.

5.2 Genus fluctuations influence on the false vacuum decay

If spacetime fluctuations are not taken into account, the vacuum decay rate is given by $e^{-B_{seed}}$. However, if the effects of genus fluctuations are considered, there are different ways in which vacuum decay can occur. In the decay from the false vacuum state to the true vacuum state, the spacetime may produce various genus. All these possible variations in spacetime must be taken into consideration. Therefore, when accounting for genus fluctuations, the vacuum decay rate should be adjusted to equation (69).

Comparing equations (69) and (84), one can find that the relationship between the vacuum decay rate Γ_{tot} and the genus $g-1$ tunneling rate $\Gamma(g-1)$ is given by

$$\Gamma_{tot} = e^{-B_{seed}} + e^{-B_{seed}} \sum_{g=2}^{\infty} \Gamma(g-1). \quad (93)$$

Substituting equation (87) into (93), one can obtain

$$\Gamma_{tot} = \frac{2\Xi(\phi_2) + 1}{2\Xi(\phi_2)} e^{-B_{seed}} \text{LerchPhi}\left[\Theta(\phi_2) \text{erfi}\left(\frac{1}{2}\sqrt{\pi\Xi(\phi_2)}\right), 1, \frac{2\Xi(\phi_2) + 1}{2\Xi(\phi_2)}\right], \quad (94)$$

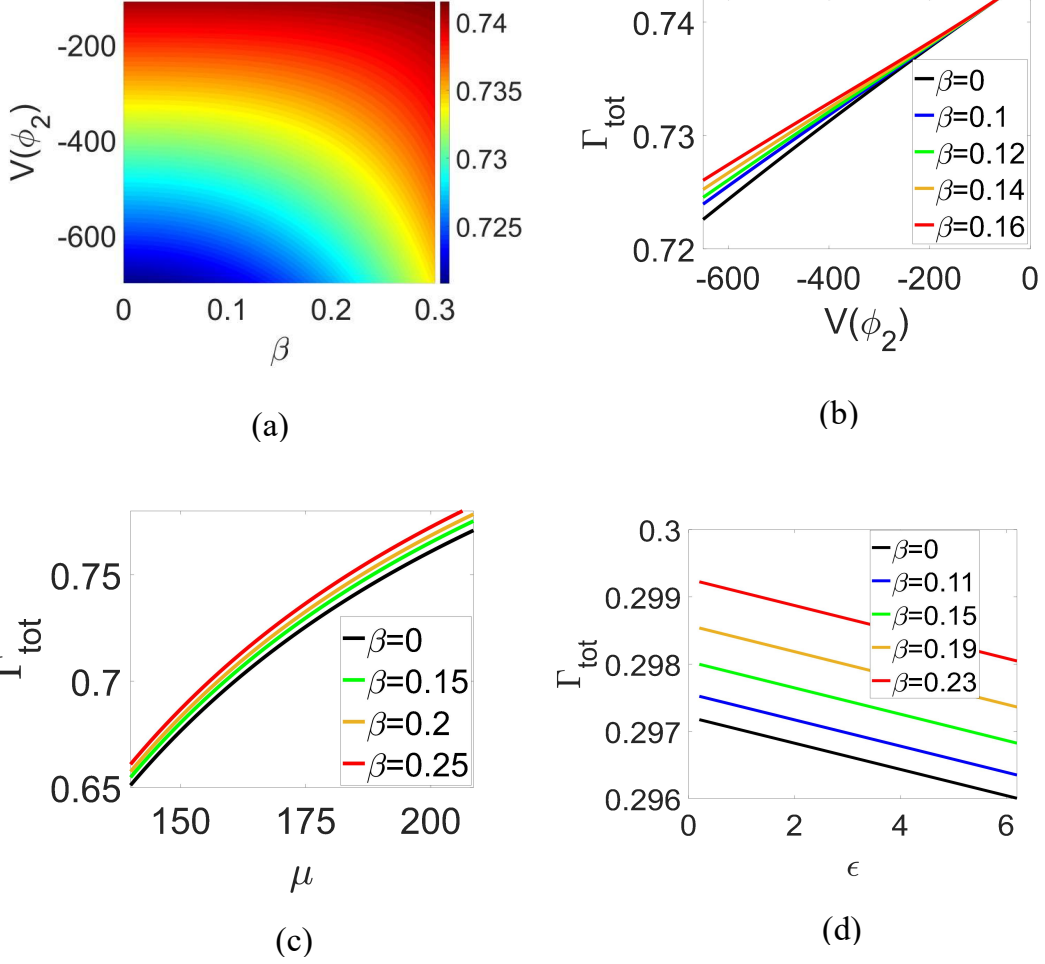


Figure 10: Variations in the vacuum decay rate Γ_{tot} under the condition $\alpha = 0.2$. In figure 10 (a), the horizontal axis and the vertical axis represent the upper limit of the coupling strength Y_{12} and the false vacuum energy density $V(\phi_2)$, respectively. Different colors represent different values of the vacuum decay rate Γ_{tot} . In figures 10 (b), (c) and (d), the vertical axes represent the vacuum decay rate Γ_{tot} . The horizontal axes of figure 10 (b), (c) and (d) represent the false vacuum energy density $V(\phi_2)$, the tension of the domain wall and the difference of the two vacuum energy density, respectively. Different curves correspond to different values of the parameter β . The black curves represent the vacuum decay rate in the Coleman-De Luccia theory. The parameters are set as follows: in figures 10 (a) and (b), $\mu = 150$ and $\epsilon = 0.1$; in figure 10 (c), $V(\phi_2) = -800$ and $\epsilon = 1$; in figure 10 (d), $V(\phi_2) = -500$ and $\mu = 70$.

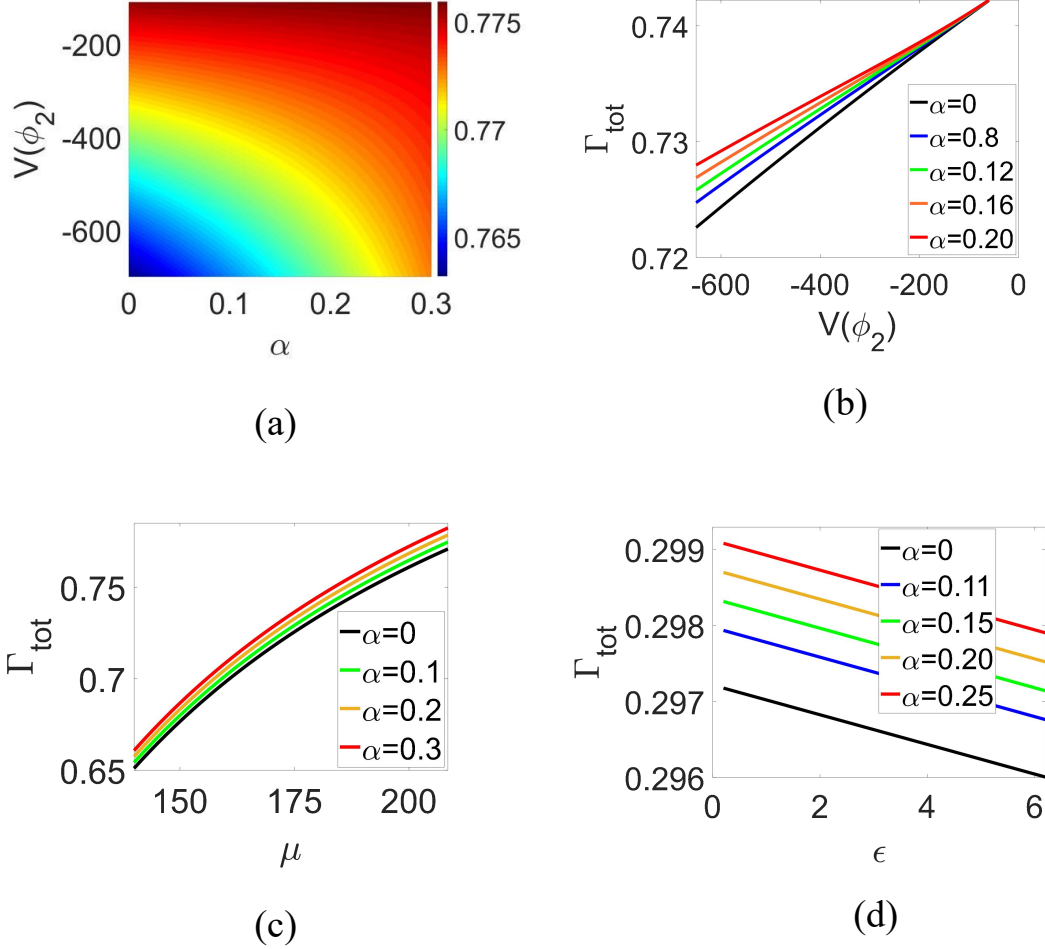


Figure 11: Variations in the vacuum decay rate Γ_{tot} under the condition $\beta = 0.2$. In figure 11 (a), the horizontal axis and the vertical axis represent the upper limit of the coupling strength Y_{12} and the false vacuum energy density $V(\phi_2)$, respectively. Different colors represent different values of the vacuum decay rate Γ_{tot} . In figures 11 (b), (c) and (d), the vertical axes represent the vacuum decay rate Γ_{tot} . The horizontal axes of figure 11 (b), (c) and (d) represent the false vacuum energy density $V(\phi_2)$, the tension of the domain wall and the difference of the two vacuum energy density, respectively. Different curves correspond to different values of the parameter α . The black curves represent the vacuum decay rate in the Coleman-De Luccia theory. The parameters are set as follows: in figure 11 (a), $\mu = 200$ and $\epsilon = 0.1$; in figure 11 (b), $\mu = 170$ and $\epsilon = 0.1$; in figure 11 (c), $V(\phi_2) = -800$ and $\epsilon = 1$; in figure 11 (d), $V(\phi_2) = -500$ and $\mu = 70$.

where,

$$\text{LerchPhi}[x, s, a] \equiv \sum_{n=0}^{\infty} \frac{x^n}{(a+n)^s} \quad (95)$$

is the Lerch transcendent function [60]. In equation (94), the factor $e^{-B_{seed}}$ is the vacuum decay rate as predicted by the Coleman-De Luccia theory, while the other factors represent the contribution of the genus fluctuations.

Figure 10 shows the variations in the vacuum decay rate Γ_{tot} . Figures 10 (a) and (b) show that as the absolute value of the false vacuum energy density decreases, the vacuum decay rate Γ_{tot} increases. Figure 10 (b) indicates that as $|V(\phi_2)|$ decreases, different curves will intersect at one point, implying that the effects of the genus fluctuations decrease as $|V(\phi_2)|$ decreases. This result aligns with the result from figures 8 (b), (c) and figure 9 (a). Figure 10 (b) also indicates that the vacuum decay rate Γ_{tot} increases with $V(\phi_2)$. In our model, a smaller $V(\phi_2)$ (keeping other parameters fixed) may correspond to a higher potential barrier between the two vacuum states. Thus, figure 10 (b) implies that a higher potential barrier corresponds to a harder tunneling. This is a typical feature of various quantum tunneling processes.

Figure 10 (c) reveals that as the tension of the domain wall increases, the vacuum decay rate Γ_{tot} also increases. Furthermore, figure 10 (d) shows that a smaller energy density difference between the false vacuum state and the true vacuum state corresponds to a higher vacuum decay rate. The black curves in figures 10 (b), (c) and (d) represent the variations in the vacuum decay rate without genus fluctuations. These figures indicate that considering the effects of the genus fluctuations will lead to an increase in the vacuum decay rate. This is because accounting for genus fluctuations means that more possible ways of vacuum decay are considered. Figures 9 (b) and 10 (a), 10 (b), 10 (c) and 10 (d) illustrate that the precise value of parameter β has no impact on any qualitative conclusions. Figure 11 is similar to figure 10, indicating that the particular value of parameter α also has no influence on the qualitative results.

6 Conclusions and discussions

In this work, we studied the genus fluctuations of the AdS₃ spacetime and its influence on the false vacuum decay. Our model consists of a real scalar field coupled with the

three dimensional spacetime. The scalar potential has two minimal values, corresponding to two vacuum states. In the Coleman-De Luccia theory, the vacuum decay rate is determined by the total tunneling action. This action consists of the Euclidean action of the bounce solution and the background term. Under the thin wall approximation, the bounce solution can be visualized as a spherically symmetric bubble embedded in the sea of false vacuum. Thus, the total tunneling action can be divided into three components: the tunneling action inside, within and outside the domain wall. For convenience, we define the vacuum decay seed as the tunneling action inside and on the domain wall. In the absence of genus fluctuations, the tunneling action outside of the bubble is zero. Therefore, in this scenario, the total tunneling action is equivalent to the vacuum decay seed.

We demonstrate that the tunneling action outside of the bubble is non-zero in the presence of genus fluctuations. The volume of the AdS_3 spacetime is infinite. Thus, when studying the tunneling action outside the bubble, the volume and the action of the spacetime should be regularized. Both the regularized action and the original Einstein-Hilbert action correspond to the same spacetime dynamical equation.

We categorize the genus fluctuations into three classes. In the first class, both ends of the wormhole are inside the bubble. In the second class, only one end of the wormhole is inside the bubble. In the third class, both ends of the wormhole are outside of the bubble. The third class of fluctuations does not affect the vacuum decay seed. Our focus is on the scenario where the radius of the bubble is much smaller than the size of the AdS_3 spacetime. In this case, the third class of fluctuations is predominant. Thus, we disregard the first and second classes of fluctuations.

The three dimensional high genus spacetime includes handlebodies and non-handlebodies. Some researchers argue that the effects of the handlebodies are predominant. Thus, for simplicity, we focus on the contributions of the handlebodies. All three dimensional handlebodies can be obtained by filling the interior of a closed high genus Riemann surface. Therefore, summing over different handlebodies is equivalent to summing over various closed Riemann surfaces. There are different methods to classify the closed Riemann surfaces. Both Schottky space and the Siegel upper half space can be used to parameterize different closed Riemann surfaces. The summation over different closed

Riemann surfaces translates into an integration in these two spaces.

The regularized action of the high genus AdS_3 spacetime in Schottky space is helpful for us to derive the tunneling action of the high genus spacetime. Thus, at first, we formulate the tunneling action in Schottky space. However, it is easier to define the integral domain in the Siegel upper half space. Therefore, we transform the tunneling action from the Schottky space into the Siegel upper half space. This transformation can be simplified by the dilute wormhole gas approximation.

In the Siegel upper half space, various handlebodies are characterized by different period matrices. The off-diagonal elements are interpreted as the interactions between different wormholes or between the parent universe and the wormholes. Under the dilute wormhole gas approximation, the interactions between different wormholes are small. However, this does not imply that the interactions between the parent universe and the wormholes are also necessarily small. To simplify the tunneling action, we assume that the interactions among different wormholes are significantly smaller compared to the interactions between the parent universe and the wormholes.

Different handlebodies can be interpreted as various genus fluctuations. We show that the genus fluctuations are more likely to occur in AdS_3 spacetime with a more negative cosmological constant. We find that the fatter wormhole is easier to be created than the thin wormhole. The summation over different genus fluctuations involves an integration in the Siegel upper half space. We demonstrate that the integral domain is a subspace of the fundamental domain of the modular group $\text{Sp}(2g, \mathbb{Z})$ in the Siegel upper half space. Upon completing the integration, we obtain the tunneling rate from the genus zero spacetime state to the high genus spacetime state. We find that as the genus number increases, the tunneling rate decreases rapidly. Thus, the primary fluctuations are the one genus fluctuations. Taking into account the genus fluctuations, the vacuum decay rate will increase. In our model, despite there being two unfixed parameters, we have demonstrated that the specific values of these parameters do not affect any qualitative results.

Acknowledgements

Hong Wang was supported by the National Natural Science Foundation of China Grant No. 21721003. No.12234019. Hong Wang thanks for the help from Professor Erkang Wang.

References

- [1] S. W. Hawking, Wormholes in spacetime, *Phys. Rev. D* **37** (1988) 904.
- [2] M. Lachièze-Rey and J. P. Luminet, Cosmic topology, *Phys. Rep.* **254** (1994) 135.
- [3] A. Anderson and B. S. DeWitt, Does the topology of space fluctuate?, *Found. Phys.* **16** (1986) 91.
- [4] E. Witten, Topology changing amplitudes in (2+1)-dimensional gravity, *Nucl. Phys. B* **323** (1989) 113.
- [5] S. Carlip and R. Cosgrove, Topology change in (2+1)-dimensional gravity, *J. Math. Phys.* **35** (1994) 5477.
- [6] S. Carlip and S. P. De Alwis, Wormholes in 2+1 dimension, *Nucl. Phys. B* **337** (1990) 681.
- [7] B. Bahr, On background-independent renormalization of spin foam models, *Class. Quant. Grav.* **34** (2017) 075001.
- [8] E. Witten, (2+1)-Dimensional gravity as an exactly soluble system, *Nucl. Phys. B* **311** (1988) 46.
- [9] S. Carlip, Spacetime foam: a review, *Rept. Prog. Phys.* **86** (2023) 066001.
- [10] X. Yin, Partition functions of three-dimensional pure gravity, *Commun. Num. Theor. Phys.* **2** (2008) 285.
- [11] X. Yin, On non-handlebody instantons in 3D gravity, *JHEP* **09** (2008) 120.

- [12] H. Maxfield, S. F. Ross and B. Way, Holographic partition functions and phases for higher genus Riemann surfaces, *Class. Quantum Grav.* **33** (2016) 125018.
- [13] S. Carlip, The sum over topologies in three-dimensional Euclidean quantum gravity, *Class. Quant. Grav.* **10** (1993) 207.
- [14] K. Krasnov, Holography and Riemann surfaces, *Adv. Theor. Math. Phys.* **4** (2000) 929.
- [15] L. A. Takhtajan and L.-P. Teo, Liouville action and Weil-Petersson metric on deformation spaces, global Kleinian reciprocity and holography, *Commun. Math. Phys.* **239** (2003) 183–240.
- [16] J. Park, L. A. Takhtajan and L.-P. Teo, Potentials and Chern forms for Weil–Petersson and Takhtajan–Zograf metrics on moduli spaces. *Adv. Math.* **305** (2017) 856–894.
- [17] J. Park and L.-P. Teo, Liouville action and holography on Quasi-Fuchsian deformation spaces, *Commun. Math. Phys.* **362** (2018) 717–758.
- [18] A. Maloney and E. Witten, Quantum gravity partition functions in three dimensions, *JHEP* **02** (2010) 029.
- [19] N. Iizuka, A. Tanaka and S. Terashima, Exact path integral for 3D quantum gravity, *Phys. Rev. Lett.* **115** (2015) 161304.
- [20] S. Coleman, Why there is nothing rather than something: a theory of the cosmological constant, *Nucl. Phys. B* **310** (1988) 643.
- [21] K. Skenderis and B. C. van Rees, Holography and wormholes in 2+1 dimensions, *Commun. Math. Phys.* **301** (2011) 583–626.
- [22] A. Maloney and E. Witten, Averaging over Narain moduli space, *JHEP* **10** (2020) 187.
- [23] J. Cotler, K. Jensen and A. Maloney, Low-dimensional de Sitter quantum gravity, *JHEP* **06** (2020) 048.

- [24] S. Collier and A. Maloney, Wormholes and spectral statistics in the Narain ensemble, JHEP **03** (2022) 004.
- [25] H. Zolfi, Complexity and multi-boundary wormholes in 2 + 1 dimensions, JHEP **04** (2023) 076.
- [26] P. Saad, S. H. Shenker and D. Stanford, JT gravity as a matrix integral, arXiv:1903.11115.
- [27] H. Zolfi, Complexity and multi-boundary wormholes in 2 + 1 dimensions, JHEP **04** (2023) 076.
- [28] B. Körs and M. G. Schmidt, Two loop Feynman diagrams in Yang-Mills theory from bosonic string amplitudes, arXiv:hep-th/0003171.
- [29] P. D. Vecchia, F. Pezzella, M. Frau, K. Hornfeck, A. Lerda and A. Sciuto, N point g loop vertex for a free Bosonic theory with vacuum charge Q, Nucl. Phys. B **322** (1989) 317.
- [30] L. Ford, Automorphic functions, Chelsea (1951).
- [31] S. Playle, Deforming super Riemann surfaces with gravitinos and super Schottky groups, JHEP **12** (2016) 035.
- [32] M. Schlichenmaier, An Introduction to Riemann Surfaces, Algebraic Curves and Moduli Spaces, Berlin: Springer-Verlag (1989).
- [33] E. D. Belokolos, A. I. Bobenko, V. Z. Enolski, A. R. Its and V. B. Matveev, Algebro-geometric approach to nonlinear integrable equations, Springer, New York (1994).
- [34] L. Magnea, S. Playle, R. Russo and S. Sciuto, Two-loop Yang-Mills diagrams from superstring amplitudes, JHEP **06** (2015) 146.
- [35] S. Coleman and K. Lee, Escape from the menace of the giant wormholes, Phys. Lett. B **221** (1989) 242.

- [36] D. C. Dai, D. Minic and D. Stojkovic, New wormhole solution in de Sitter space, *Phys. Rev. D* **98** (2018) 124026.
- [37] A. Lyons and S. W. Hawking, Wormholes in string theory, *Phys. Rev. D* **44** (1991) 3802.
- [38] H. Maaß, *Siegel's Modular Forms and Dirichlet Series*, Springer, Heidelberg Germany (1971).
- [39] N. Lu, A simple presentation of the Siegel modular groups, *Lin. Algebra Appl.* **166** (1992) 185.
- [40] J. R. Espinosaa and J.-F. Fortin, Vacuum decay actions from tunneling potentials for general spacetime dimension, *JCAP* **02** (2023) 023.
- [41] S. R. Coleman and F. De Luccia, Gravitational effects on and of vacuum decay, *Phys. Rev. D* **21** (1980) 3305.
- [42] H. Wang and J. Wang, Quantum master equation for the vacuum decay dynamics, *JHEP* **09** (2023) 113.
- [43] C. Kiefer, *Quantum gravity*, Oxford University Press, Oxford, U.K. (2007).
- [44] H. Wang and J. Wang, Quantum cosmology of the flat universe via closed real-time path integral, *Eur. Phys. J. C* **82** (2022) 1172.
- [45] H. Wang and J. Wang, Quantum geometrical current and coherence of the open gravitation system: loop quantum gravity coupled with a thermal scalar field, *Phys. Scr.* **98** (2023) 045303.
- [46] V. A. Rubakov and D. S. Gorbunov, *Introduction to the theory of the early universe*, World Scientific, Singapore (2017).
- [47] S. K. Blau, E. I. Guendelman and A. H. Guth, Dynamics of false-vacuum bubbles, *Phys. Rev. D* **35** (1987) 1747.

- [48] L. Takhtajan and P. Zograf, On uniformization of Riemann surfaces and the Weyl-Peterson metric on Teichmüller and Schottky spaces, *Math. USSR Sbornik* **60** (1988) 297-313.
- [49] S. Giombi, A. Maloney and X. Yin, One-loop partition functions of 3D gravity, *JHEP* **08** (2008) 007.
- [50] X. G. Liu and G. J. Ding, Neutrino masses and mixing from double covering of finite modular groups, *JHEP* **08** (2019) 134.
- [51] F. Diamond and J. M. Shurman, A first course in modular forms, *Grad. Texts Math.* **228**, Springer, New York, NY, U.S.A. (2005).
- [52] G. J. Ding, S. F. King and X. G. Liu, Modular A_4 symmetry models of neutrinos and charged leptons, *JHEP* **09** (2019) 074.
- [53] M. Nakahara, *Geometry, topology and physics*, CRC press, Boca Raton, US (2003).
- [54] F. Mandl and G. Shaw, *Quantum field theory*, Wiley, New York (1988).
- [55] J. Manschot, AdS₃ partition functions reconstructed, *JHEP* **10** (2007) 103.
- [56] N. Koblitz, *Introduction to Elliptic Curves and Modular Forms*, Springer-Verlag, Heidelberg Germany (1984).
- [57] S. P. De Alwis, F. Muia, V. Pasquarella and F. Quevedo, Quantum transitions between Minkowski and de Sitter spacetimes, *Fortschr. Phys.* **68** (2020) 2000069.
- [58] E. J. Weinberg, “Classical solutions in quantum field theory : Solitons and Instantons in High Energy Physics,” *Cambridge Monographs on Mathematical Physics*, September (2012).
- [59] H. Wang, Y. X. Wu, R. Li and J. Wang, Wormhole influence on the false vacuum bubble tunneling, arXiv:2310.00284v1.
- [60] L. M. Navas, F. J. Ruiz and J. L. Varona, Asymptotic behavior of the Lerch transcendent function, *J. Approx. Theory* **170** (2013) 21–31,